University of Miami
Scholarly Repository

Open Access Theses | Electronic Theses and Dissertations

2012-04-30

MRI Simulation by the EFNMR System and MatLab for Medical Imaging Teaching

Zhuang Nie
University of Miami, z.nie2010@gmail.com

Follow this and additional works at: https://scholarlyrepository.miami.edu/oa_theses

Recommended Citation
Nie, Zhuang, "MRI Simulation by the EFNMR System and MatLab for Medical Imaging Teaching" (2012). *Open Access Theses*. 321.
https://scholarlyrepository.miami.edu/oa_theses/321

This Open access is brought to you for free and open access by the Electronic Theses and Dissertations at Scholarly Repository. It has been accepted for inclusion in Open Access Theses by an authorized administrator of Scholarly Repository. For more information, please contact repository.library@miami.edu.

www.manaraa.com

UNIVERSITY OF MIAMI

MRI SIMULATION BY THE EFNMR SYSTEM AND MATALB FOR MEDICAL IMAGING TEACHING

By

Zhuang Nie

A THESIS

Submitted to the Faculty
of the University of Miami
in partial fulfillment of the requirements for
the degree of Master of Science

Coral Gables, Florida

May 2012

www.manaraa.com

©2012
Zhuang Nie
All Rights Reserved

www.manaraa.com

UNIVERSITY OF MIAMI

A thesis submitted in partial fulfillment of
the requirements for the degree of
Master of Science

MRI SIMULATION BY THE EFNMR SYSTEM AND MATALB FOR MEDICAL IMAGING TEACHING

Zhuang Nie

Approved:

_____ Weizhao Zhao, Ph.D. Associate Professor of Biomedical Engineering	_____ Terri A. Scandura, Ph.D. Dean of the Graduate School
_____ Jorge Bohorquez, Ph.D. Assistant Professor of Biomedical Engineering	_____ Kyle R.Padgett, Ph.D. Research Assistant Professor Department of Radiation Oncology

www.manaraa.com

NIE, ZHUANG (M.S., Biomedical Engineering)

MRI Simulation by the EFNMR System and MatLab for Medical Imaging Teaching. (May 2012)

Abstract of a thesis at the University of Miami.

Thesis supervised by Professor Weizhao Zhao.
No. of pages in text. (78)

Magnetic Resonance Imaging (MRI) is a fast growing medical imaging technique. Biomedical engineers will find more and more opportunities in this field. There is a growing demand of an effective teaching system for training engineering students to learn principle knowledge and have hands on experience for MRI. The objective of this research project is to cast a MRI teaching demonstration system in the laboratory environment and assist student to learn MRI through interactive simulations in the Internet accessible learning environment.

The first part of the work is to customize the newly installed EFNMR (Earth Field Nuclear Magnetic Resonance) system in the Bioimaging Lab to demonstrate nuclear magnetic resonance (NMR) phenomenon, NMR relaxation and T_1/T_2 weighted contrast mechanisms under laboratory environment. This demo is performed in the Earth's magnetic field with a low field coil probe. Procedures to acquire and optimize MRI signal, estimate/calculate T_1 and T_2 values are presented. Relaxation time T_1/T_2 weighted images are also presented.

The second part is to build two graphical user interface (GUI) platforms to simulate the magnetic resonance imaging reconstruction process. Assuming an ideal noiseless condition is setup and the Magnetic Resonance signal intensity is proportional to the

www.manaraa.com

image pixel intensity. The GUI-based simulation provides students online demonstrations of combined resonance signal, K-space construction, and FFT used to decompose signal from frequency domain back to spatial domain in an interactive fashion.

www.manaraa.com

Acknowledgements

Though this thesis is an individual work, I would never have been able to finish it without the guidance of my committee members, help from my friends and support from my family.

First and foremost, I am sincerely and heartily thankful to my thesis advisor, Dr. Weizhao Zhao, for providing me the opportunity to do this research project. Without his patient and excellent guidance, this study would not have been possible.

I would also like to thank my committee members Dr. Jorge Bohorquez and Dr. Kyle R.Padgett for their invaluable suggestions and constructive comments regarding my thesis. I would like to thank Wupeng Yin, who as a good friend was always willing to help and give her best suggestions. Besides, thanks to all my friends in the Medical Imaging Lab, Che Liu, Jian Fang, Hairong Chen. It is a great pleasure to thank everyone who helped me during my work.

Finally, and most importantly, I would like to express my deepest appreciate and love to my parents and all the family members. Without their unconditional love and support, I will not have this life-changing opportunity to study abroad and accomplish this thesis.

Zhuang Nie

May 2012, Miami

www.manaraa.com

Table of Contents

List of Figures vi

List of Tables xii

Chapter 1 Introduction 1

Chapter 2 MRI Background Introduction 5

Magnetic Field 6

RF Coil 7

Magnetic Resonance (MR) Signal 8

Magnetic Resonance Gradient System 14

Chapter 3 The Earth's Field Magnetic Resonance System 20

Earth's Magnetic Field 20

EFNMR System Components 20

EFNMR Magnetization 23

Excitation Pulse 25

Pulse Sequence 26

Chapter 4 EFNMR Experiment 29

Experimental Samples 29

Parameters Initialization 29

Magnetic Resonance (MR) Signal Collecting 35

www.manaraa.com

Measurements of Relaxation times 37

T1 Measurement 39

T2 Measurement 41

Relaxation Time Weighted Effect Image 43

Chapter 5 Graphical User Interface Tutorial 50

Magnetic Resonance Signal Tutorial 50

Reconstruction Simulation 56

Chapter 6 Conclusion 58

Reference 60

APPENDIX 64

www.manaraa.com

List of Figures

Figure 2. 1 MRI produced by GE. 5

Figure 2. 2 Superconducting magnets. 6

Figure 2. 3 A charged spin. 9

Figure 2. 4 A charged spin precessing along the external magnetic field. 9

Figure 2. 5 The reference frame system. The Z axis refers to the longitudinal direction. The X-Y plane refers to the transverse plane. 10

Figure 2. 6 The excitation RF pulse with resonance frequency is applied perpendicular to the external magnetic field B_0. The net magnetization M_0 will be tipped down to the X-Y plane by the RF pulse. 11

Figure 2. 7 The flip angle $\boldsymbol{\alpha}$ reflects the degree to which the net magnetization be flipped down relative to the longitudinal axis. 12

Figure 2. 8 The first figure shows the re-growth of magnetization along the Z axis (from blue to red). The second figure shows the decay of magnetization in the X-Y plane (from red to blue). 13

Figure 2. 9 The Free Induction Decay (FID) signals are received by the receiver coil. ... 14

Figure 2. 10 Time of repeat (TR) is the duration interval between two RF pulses. 17

Figure 2. 11 The partial saturation pulse sequence and saturation pulse sequence are constituted only by 90 ˚ RF pulses. The different is the TR parameter. 17

Figure 2. 12 The inversion recovery sequence. 18

www.manaraa.com

Figure 2. 13 A normal single echo Spin Echo pulse sequence. TE is interval between the excitation pulse and echo acquisition. 19

Figure 3. 1 The probe used in the experiment. It consists of three sets of coil. 21

Figure 3. 2 The three sets of coils: B1 coil, Gradient Coil and Polarization Coil. 22

Figure 3. 3 The digital signal processor. It controls the probe. 22

Figure 3. 4 The flow chart describes the whole working process of the EFNMR system. 23

Figure 3. 5 The polarization field is applied perpendicular to the Earth's magnetic field. 23

Figure 3. 6 Hydrogen nuclear spins of the sample in the nature state. They are random direction. 24

Figure 3. 7 After the application of polarization field Bp, all spins aligned along the Bp direction. 24

Figure 3. 8 The wooden stand that supports the probe. 26

Figure 3. 9 In the EFNMR experiment, configure these timing parameters to control the pulse sequences. Timing parameters include: pulse duration, TR and TE. Pulse duration is the time that pulse is applied. TR is the time interval between two successive pulses. TEis the time interval between the excitation pulse and the Magnetic Resonance (MR) signal measurement. 26

Figure 3. 10 The pulse sequence used in Earth's field experiment to acquire a signal. The second floor shows the evolvement of the magnetization direction. 27

www.manaraa.com

Figure 4. 1 The curve of resonance frequency versus capacitance 30

Figure 4. 2 Autotune experiment 30

Figure 4. 3 The 2D figure of the Echo Signal versus Capacitance 31

Figure 4. 4 The excitation pulse produced by the B1 coil flips the nuclear magnetization with a flip angle α to the transverse plane. 32

Figure 4. 5 The parameter set of B1 Duration experiment. 32

Figure 4. 6 This plot is the transverse magnetization VS the B1 Duration. 34

Figure 4. 7 The parameter set of FID collection experiment. 35

Figure 4. 8 The free induction decay (FID) signal get in the project. It shows the decay process of the magnetization in the transverse plane. 36

Figure 4. 9 Spin echo pulse sequence parameter set. 36

Figure 4. 10 The echo signal. It shows the regrowth process after the application of refocus pulse. 37

Figure 4. 11 The parameter set for $\boldsymbol{T1}$ measurement. 39

Figure 4. 12 The plot of $\boldsymbol{T1}$ curves. The red line is water and the blue line is copper sulfate solution. 41

Figure 4. 13 The parameter set of spin echo pulse sequence for $\boldsymbol{T2}$ measurement. 41

Figure 4. 14 The plot of $\boldsymbol{T2}$ curves. The red line is water and the blue line is copper sulfate solution. 43

www.manaraa.com

Figure 4. 15 When polarization duration smaller than 1500 ms will produce the most significance difference of the signal amplitude. When polarize duration is more than 3000 ms, it tends to have no difference. 45

Figure 4. 16 The smaller the echo time, the less difference. The echo difference between the two samples is proportional to the echo time. With the increasing of echo time, the difference is increase too. 46

Figure 4. 17 Parameter set for $\boldsymbol{T1}$ weighted image. 47

Figure 4. 18 This is the image result to simulate the $\boldsymbol{T1}$ weighted effect image. The FOV of this image is 120*120 mm. Polarization duration is 1300 ms, echo time is 210 ms. In this image, the copper sulfate is brighter than the water..... 47

Figure 4. 19 Parameter set for $\boldsymbol{T2}$ weighted image. 48

Figure 4. 20 This is the image result to simulate the $\boldsymbol{T2}$ weighted effect image. The FOV of this image is 120*120 mm. Polarization duration is 3000 ms, echo time is 320 ms. In this image, the water is brighter than the copper sulfate..... 48

Figure 5. 1 The Magnetic Resonance Signal Tutorial. All simulation in this tutorial is based on the 3by3 matrix. From the perspective of function, this tutorial GUI is separated into five parts. 51

Figure 5. 2 This is Part A of the GUI tutorial. User can set the elements value of the matrix and other parameters: base frequency, frequency gradient, sampling time. User should notice that the base frequency should larger than the frequency gradient. The grayscale image is also shown below. 52

www.manaraa.com

Figure 5. 3 This is part B of the GUI tutorial. The simulated magnetic resonance signals and their combination is shown. Fourier transform is applied to discompose the combined magnetic resonance signal. 53

Figure 5. 4 These are Part C, Part D and Part E of the GUI tutorial. In Part C displays the simulated magnetic resonance signal in time domain and frequency domain. Part D is the result of data domain. Part E includes the reconstructed grayscale image and the matrix. 55

Figure 5. 5 This is reconstruction simulation GUI. User can choose the image and play the whole simulation process with the chosen image. User can see the simulated signal in time domain and frequency domain in the left side. K-space of the image and the reconstruction result are displayed in the right side..... 56

Figure 5. 6 This is an example with a stomach image. User can see the simulated signal in time domain and frequency domain in the left side. K-space of the image and the reconstruction result are displayed in the right side..... 57

Figure 1 Analyses B1 coil..... 64

Figure 2 Experiment1 result and LCR circuit..... 65

Figure 3 Find Resonance frequency 66

Figure 4 Experiment 2 result..... 66

Figure 5 Acquire free induction decay..... 67

Figure 6 Experiment 3 result..... 68

Figure 7 Experiment 4 and result..... 69

www.manaraa.com

Figure 8 Get the B1 duration parameters 70

Figure 9 Experiment 5 result..... 71

Figure 10 Acquire the spin echo signal..... 72

Figure 11 Deshim process..... 72

Figure 12 Experiment 6 result..... 73

Figure 13 Relaxation time measurement experiment 74

Figure 14 Experiment 7 result..... 75

Figure 15 Relaxation time measurement experiment 75

Figure 16 Experiment 8 result..... 76

Figure 17 Gradient echo imaging 77

Figure 18 Experiment 9 result-1 78

Figure 19 Experiment 9 result-2 78

www.manaraa.com

List of Tables

Table 1 The experiment result of different pulse duration and the corresponding transverse magnetization. All the result transverse magnetization is recorded in the second row. 33

Table 2 This table shows the resulting magnetization amplitude VS polarization duration. The left column is the result for water. The right column is the result for copper sulfate solution. 40

Table 3 This table shows the resulting echo signal amplitude of the different echo time. The left column is the data result of water. The right column is the data result of the copper sulfate solution. 42

www.manaraa.com

Chapter 1 Introduction

Magnetic Resonance Imaging (MRI) has been a clinical application for only the past few decades, but the evolvement of the technique has been over a century [1]. The remarkable works by many great scientists from different fields have contributed to the development of MRI. Nikola Tesla invented the Tesla coil in 1891 [2]. Irish physicist Sir Joseph Larmor who lived in the 19th century explained the famous Larmor equation [3]. The year 1946 was an important time for MRI. In this year, the nuclear magnetic resonance signal was discovered independently by Felix Bloch and Edward Purcell [4-6]. Another important time for MRI is year 1974, Paul C. Lauterbur and Peter Mansfield independently figured out the method to get the spatial information of the nuclear magnetic resonance signals originated within the sample [7, 8]. This invention is the foundation for converting NMR signal to two-dimensional magnetic resonance imaging. In 1975, Richard Ernst used the Fourier transform method to rapidly reconstruct an image from nuclear magnetic resonance signals [9, 10]. This method is the basis of today's reconstruction algorithm.

With the above theoretical basis, the first commercial Magnetic Resonance Imaging (MRI) scanner was produced by FONAR in 1980s. This non-invasive, non-ionizing radiation imaging modality has had rapidly developed in the last thirty years. This high soft-tissue resolution imaging technique is able to not only provide anatomical information but also functional information. With the special advantages, Magnetic Resonance Imaging (MRI) is widely applied, including tumor detection [11],

www.manaraa.com

cardiovascular MR [12], anatomical and functional imaging of brain [13, 14], two and three dimensional MR angiography [15, 16], real time imaging [17] and so on. MRI is now a routine examination in hospital. According to the data from the European Magnetic Resonance Forum (EMRF), it is estimated there are about 10,000 MRI units in USA. This number is still growing. At the same time, opportunities in this field are plentiful.

MRI results from integration of multidisciplinary knowledge and combination of multiple techniques. For example, the hydrogen spinning is a quantum mechanics property which involves knowledge in the quantum physics field. The nuclear magnetic resonance signal is a physicochemical phenomenon which involves the knowledge of physical chemistry. The Tesla coil used in MRI is an induction coil which involves the knowledge in the radio technology. Magnetic field gradient technique to map the MR signal distribution involves the knowledge in electromagnetic field. The mathematical transformation method used for magnetic resonance signal analysis and image reconstruction. Besides, the principle of MRI also includes some complicated process and abstract concepts. Such as, the relaxation process is a complex quantum physics phenomenon in proton particle scale. Another complex process is the imaging pulse sequence, which is referred as the tool to acquire the MR signals. K-space is the abstract notion that describes the middle state between MR signals and reconstructed image. The multidisciplinary knowledge, complicated process and abstract concepts make MRI a complex system. [6, 18-20]

MRI is not only a complex system but also with a huge market. More and more engineers, physicists, chemists and scientists in other fields are involved in MRI's research,

www.manaraa.com

application and manufacture. So there is a demand: how to get an effective training system for such a complex system? We all know that MRI is a million valued price of equipment. It is impractical to have a learner be trained with a real one. So simulation is the alternative method. For example, many institutes have produced MRI tutorial website with pictures and animations to show the principles of MRI.

Our hypothesis is that an accessible interactive system will be more effective than conventional demonstration. In this research project, the work is committed to cast an interactive MRI simulation system in the laboratory environment to help the engineering students learn the basic principles of MRI. This MRI simulation system consists of hardware and software systems. For the hardware system, a coil probe that works on the Earth's magnetic field is utilized. The system is a very low cost substitute of real MRI. Students can easily access this device in the laboratory and perform real nuclear magnetic experiments on it. For the software system, an easy to use graphical user interface based on MATLAB is designed to simulate the MR signal processing and reconstruction process. The combination of these two forms an effective way to demonstrate the principles of MRI.

The thesis is arranged as follows. In chapter 2 a brief overview of the basic concepts of MRI is provided. Chapter 3 provides the introduction of the components and working principles of the Hardware system. In chapter 4, an Earth's magnetic field nuclear magnetic resonance (EFNMR) system was set up in the lab environment. Base on this EFNMR system, several MRI experiment was carried out, include MR signal acquisition, relaxation time parameter measurement, and the simulation of relaxation time weighted

www.manaraa.com

images. This is a good MRI technique education demo in the laboratory which is easily accessible to the students. Chapter 5 describes the work of by developing a visual and easy to use graphical user interface system to provide an interactive platform that helps students understand related magnetic resonance imaging principles and concepts. Magnetic field gradients that provide the spatial information, pulse sequence that used to acquire the MR signals, k-space that contains all the received data and Fast Fourier Transform (FFT) that used as the reconstruction algorithm are the most important concepts in magnetic resonance imaging. The GUI interactive platforms will simulate all these important concepts.

In the last chapter, we conclude that this research project focuses on developing a broadly covered and easy understanding MRI education platform for students, which can lead to an enhanced and faster absorption, comprehension of the relative concepts of the MRI.

www.manaraa.com

Chapter 2 MRI Background Introduction

Magnetic Resonance Imaging (MRI) is a noninvasively imaging technique that can produce tomographic images from human or other biological systems. MRI images are of high quality and rich information content. Relative researches have shown that with appropriate operation the magnetic field of clinical MRI has no harmful effects to human body [21-23]. With these advantages, MRI is a valuable tool in biological and medical fields.

Figure 2. 1 MRI produced by GE.

How does Magnetic Resonance Imaging work? In brief, the patient is placed in a strong and homogeneous magnetic field. A radiofrequency (RF) pulse and a gradient field around the patient are then applied to selectively excite the interested region of the patient. Received MR signals are collected and organized in a "spatial- frequency- space" called K-space. Through the DFT processing to the K-space data, the tissue structure in the interested region can be reconstructed and other useful information can also be revealed [18, 19, 24].

www.manaraa.com

Magnetic Field

Magnetic Resonance Imaging (MRI) requires a strong and uniform static magnetic field. There are mainly three types of magnets used to generate magnetic field: permanent magnets, electromagnets and superconducting magnets [25]. Permanent magnets are composed of materials that produce their own persistent magnetic fields; electromagnets produce magnetic field by the moving charges and current; superconducting magnets are electromagnets that be cooled down to near absolute zero (0˚ Kelvin or -270 C˚) to achieve no resistance situation [26]. Most commercial MRI scanners nowadays use the superconducting magnets to provide the magnetic field.

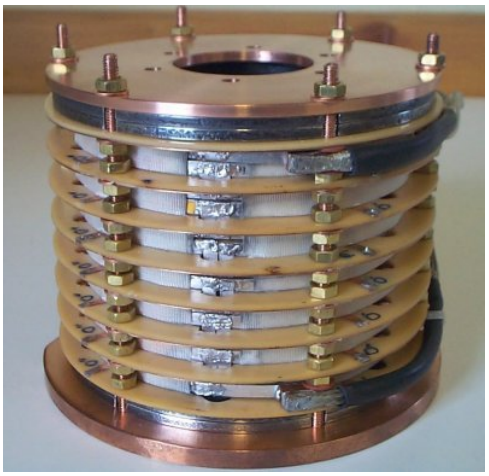

Figure 2. 2 Superconducting magnets.

The superconducting MRI magnet is produced by the wires which are wound in spiral coils. The cooling system is made up by liquid helium and liquid nitrogen. Liquid helium is the coolant for coils. Liquid nitrogen prevents the liquid helium coolant from boiling away by insulating the liquid helium coolant from any heat exchanging with the outer environment. As the spiral coils of superconducting magnets have no resistant and there

www.manaraa.com

is no energy loss, large currents can be achieved producing a very strong magnetic field. The unit of magnetic field strength is gauss (G) or tesla (T), and 1T equals 10^4 G. The magnetic strength of commercial superconducting magnets range from 1.0T up to about 11.4T, comparing to the less than 0.4T magnetic field of a permanent magnet. However, depending on the application, different field strength is chosen. Most clinical using MRI scanners use a 0.5 to 3.0T magnet field strength [27].

In practice, the main magnetic field is not homogeneous enough. An auxiliary magnetic field is applied to compensate for the inhomogeneity of the main magnetic field. This auxiliary magnetic field is produced by another set of coils which called shim coils [18].

In a typical MRI scan, the patient lies inside the spiral coils that constitute the superconducting magnet. The direction of the main magnetic field is along the longitudinal axis of the patient.

RF Coil

The function of Radiofrequency (RF) coil is either for Magnetic Resonance (MR) signal excitation or for MR signal detection [18]. By applying an alternating electric current through the RF coil, another magnetic field B1 will be generated. The B1 magnetic field is very small in magnitude comparing to the main magnetic field. Its direction is along the transverse axis of the patient that lies in the MRI, such that the magnetic field B1 is perpendicular to the external main magnetic field.

The alternating electric current that is applied to the RF coil will be turned off in a few microseconds or milliseconds to terminate the B1 magnetic field. The B1 magnetic field

www.manaraa.com

also oscillates in the particular frequency, which is ranged in the radio frequency [28]. This brief magnetic field also called Radio Frequency pulse (RF pulse).

Magnetic Resonance (MR) Signal

Unlike other tomographic imaging modalities, such as Computed Tomography (CT), Positron Emission Tomography (PET) and ultrasound imaging, in which imaging signal is produced by the external signal sources or particular substances like radioactive isotopes for PET, the detected signal in Magnetic Resonance Imaging (MRI) is coming from the exited substances of the tested object itself [18]. Dominant substance in human body is hydrogen atom [29]. For most MRI studies, the detected signal is emitted by hydrogen nuclei [18].

The nucleus is the center of an atom, composed of protons and neutrons. In quantum mechanics, nucleus, protons, and neutrons all have a fundamental characteristic property, spin. Spin is the movement that the particle rotates around its own axis. Atoms that have odd atomic weights and/ or odd atomic numbers (odd number of protons, neutrons, or proton plus neutrons) are considered as the signal source in Nuclear Magnetic Resonance Imaging, because of the "unpaired" phenomenon [26]. Hydrogen nucleus is a single proton which is positive proton. This positive charged spinning particle can produce a magnetic field, like a tiny bar magnet. This tiny bar magnet will align itself always along the direction of the external magnetic field, which is called the magnetic dipole moment (MDM) [26]. Briefly, unpaired spinning nucleus has magnetic dipole moment (MDM), which is the physics basic for MRI.

www.manaraa.com

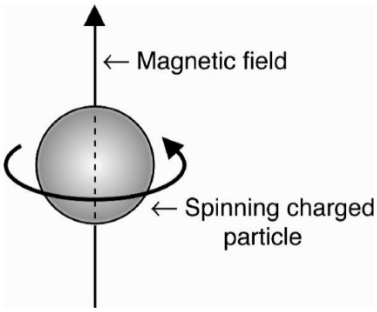

Figure 2. 3 A charged spin.

Besides, with the present of the external magnetic field, the hydrogen nuclei will not only rotate around their own axis but also their MDM will rotate around the axis of the external magnetic field. This phenomenon is called precession.

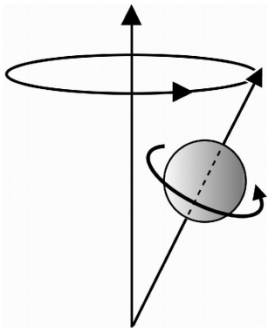

Figure 2. 4 A charged spin precessing along the external magnetic field.

The precession rate of these MDM is called precession frequency in unit of cycles per second. This frequency is directly proportional to the external magnetic field [26]. The relationship is presented by the Larmor Equation:

$$\omega = \gamma * B_0 \qquad \text{Eq. 1}$$

where ω is the Larmor frequency of the MDM in unit of radians per second, γ is the gyromagnetic ratio of this nucleus in unit of radian per second per tesla ($s^{-1} \cdot T^{-1}$), and B_0

www.manaraa.com

is the strength of the external magnetic field in unit of Tesla (T). For hydrogen, its gyromagnetic ratio is 42.6 MHz/Tesla. Under a 1.5 Tesla magnetic field, its precession frequency become 64MHz [26].

In human physiology, water is the major constituent of the human body, which accounts for two-thirds of the total weight for a normal adult [29]. Each water molecule has two hydrogen atoms. Every hydrogen nucleus possesses a magnetic dipole moment (MDM). In the natural state, the huge number of magnetic dipole moment (MDM) in the body is random distribution. When a strong external magnetic field presents, the MDM will be aligned along the direction of this main magnetic field. The accumulation of these MDMs is called net magnetization, presented by M_0, which is in the same direction as the external magnetic field.

When the patient is lying in the strong and homogeneous external magnetic field, the direction from the head to foot is along the Z axis longitudinally. Every hydrogen proton MDM is processing along the Z axis and the net magnetization M_0 is also in the Z direction. The X and Y axis direct in the transverse plane.

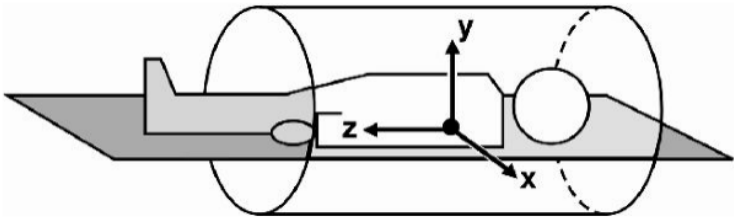

Figure 2. 5 The reference frame system. The Z axis refers to the longitudinal direction. The X-Y plane refers to the transverse plane.

www.manaraa.com

At this moment, the RF pulse is applied to the patient and its direction is in the X-Y plane. The frequency of the RF pulse is tuned to equal to the precession frequency of the hydrogen MDM, then resonance occurs. These MDMs will begin to rotate along the RF pulse. The net magnetization M_0 will be tipped down to the X-Y plane.

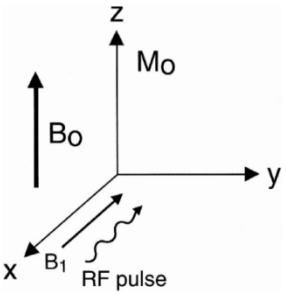

Figure 2. 6 The excitation RF pulse with resonance frequency is applied perpendicular to the external magnetic field B_0. The net magnetization M_0 will be tipped down to the X-Y plane by the RF pulse.

The flip angle α is the angle to which the net magnetization M_0 is tipped down relative to the Z axis, which defined as the flow equation:

$$\alpha = \gamma * B1 * \tau \qquad \text{Eq. 2}$$

Where γ is the hydrogen gyromagnetic ratio, B1 is the strength of the RF magnetic field generated by the RF coil and τ is the duration of the RF pulse [26]. From the equation, the flip angle is directly proportional to the amplitude and duration of the RF pulse.

www.manaraa.com

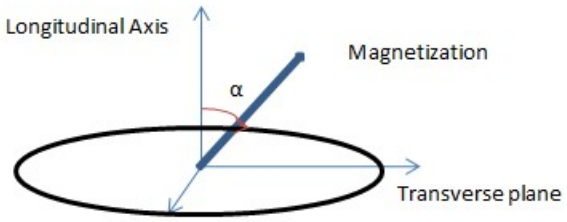

Figure 2. 7 The flip angle α reflects the degree to which the net magnetization be flipped down relative to the longitudinal axis.

If α equal to 90 ˚, the net magnetization M_0 is tipped in the X-Y plane. This pulse is known as 90 ˚ RF pulse. Another important pulse is 180 ˚ RF pulse, which invert the net magnetization M_0 to the opposite direction. Pulse sequence is the combination of these two pulses.

Mxy is the transverse component of the net magnetization M0 in the X-Y plane. While application a 90 ˚ RF pulse, Mxy will equal to net magnetization M0 and the longitudinal component of the net magnetization M_0 in the Z axis will decay to zero.

In a few microseconds, the RF pulse is terminated. The perturbed magnetization is recovering to the prior state. The re-growth of the longitudinal magnetization Mz is called longitudinal relaxation or T_1 relaxation, and the decay of the transverse magnetization Mxy is called transverse relaxation or T_2 relaxation.

www.manaraa.com

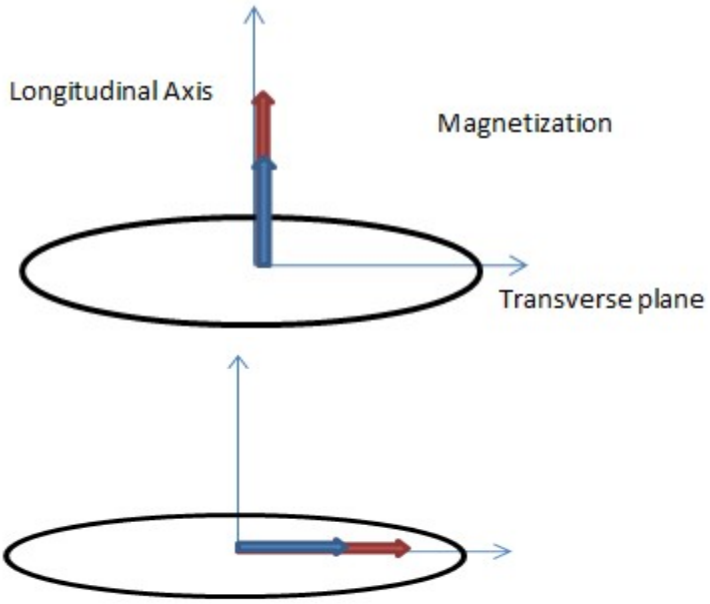

Figure 2. 8 The first figure shows the re-growth of magnetization along the Z axis (from blue to red). The second figure shows the decay of magnetization in the X-Y plane (from red to blue).

T_1 and T_2 are time constants. T_1, also known as spin-lattice relaxation time, refers to the time used for the Mz magnetization to recovery to 63% of the net magnetization M0 (Mz magnetization that before the application of the RF pulse). T_2, also known as spin-spin relaxation refers to the time used for the Mxy magnetization to decay to 37% of the net magnetization (Mxy magnetization that before the application of RF pulse). The regrowth of the Mz magnetization and the decay of the Mxy magnetization are two different but related processes with different rates, but both of them follow exponential functions.

The decay of Mxy is more rapid than the recovery of Mz, so T_1 is always longer than T_2. The values of T_1 and T_2 are characteristics of the tissue.

www.manaraa.com

The decay of transverse magnetization Mxy produces the MR signal that is used to form the MR image. This MR signal can also be received by the RF coil. The MR signal is illustrated as the figure below. It is an oscillating and decaying signal, called free induction decay (FID).

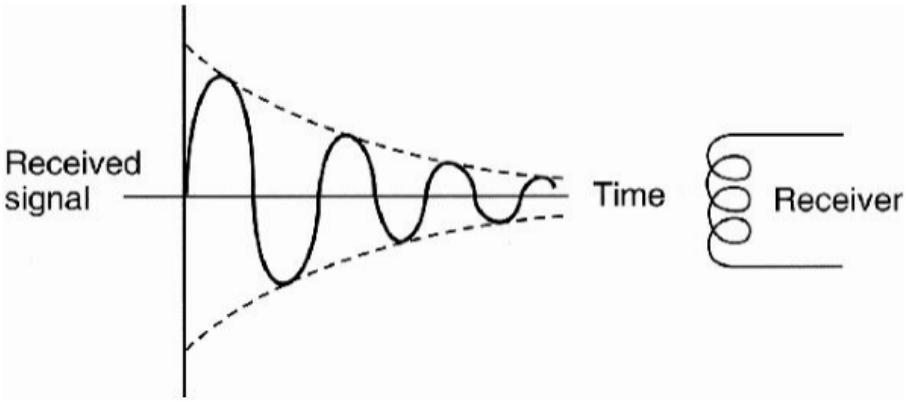

Figure 2. 9 The Free Induction Decay (FID) signals are received by the receiver coil.

The magnitude of the MR signal FID is related to the flip angle, the number of nuclear spins in the sample, the magnetic field strength and others. The decaying time of the FID is depending on the degree of field inhomogeneity. The FID signals from every parts of the whole body are collected simultaneously.

Magnetic Resonance Gradient System

The main function of magnetic resonance gradient system is to provide the spatial information of these signals. This system commonly consists of three orthogonal gradient coils. The magnetic field produced by these gradient coils is varying in space called magnetic field gradient. The gradient strength is normally measured in units of milli-tesla per meter (mT/m). Three magnetic field gradients are slice selection gradient in Z axis

www.manaraa.com

(Gz), phase encoding gradient in Y axis (Gy), and frequency encoding gradient in X axis (Gx).

The slice selection gradient Gz produces a gradual and linear change in the main magnetic field along the Z axis from the patient's head to the foot. From the Larmor equation, as the external main magnetic field is varying on spatial position Z, the MDM located from the head to the foot will have different precession frequency, presented by the below equation [30].

$$\omega(z) = \gamma * (B_0 + Gz * Z) \qquad \text{Eq. 3}$$

Based on the resonance theory, by tuning the RF pulse frequency, we can decide which part of the patient body to be imaged. The slice selection gradient Gz determines the Larmor frequency of the transverse image plane of the patient. The thickness of the transverse plane is altered by changing the range of frequencies of the RF pulse or the gradient steepness of the main magnetic field. With a greater range RF frequency or a less steep gradient of the magnetic field, a thicker plane can be selected. The slice selection gradient in Z axis is only turned on when the RF pulses are applied in the pulse cycle.

The frequency encoding gradient Gx and phase encoding gradient Gy generate a linear change magnetic field along the X and Y axis of the two dimensional transverse plane that have been selected, so the different intensity points within the plane can be located. The frequency encoding gradient Gx is turned on only when the signal is measured. The

www.manaraa.com

phase encoding gradient Gy is applied for a short of time during the pulse cycle after the application of the RF pulse.

In conclusion, the first step is to turn on the slice selection gradient Gx, to activate the interested slice plane spins and excite the signals; the next step is to encode spatial information to these signals by frequency encoding gradient and phase encoding gradient. The application of the magnetic resonance gradient system makes each region of the patient body experience a unique magnetic field. Based on the Larmor equation, each region will have a unique precession frequency, which is only related to the location information.

Pulse sequence

In practice, we need to repeat the RF pulse and the magnetic field gradient to get many magnetic resonance signals for reconstructing the MR image. The repeatedly applied sequence of RF pulses, magnetic field gradient and signal data acquisition is called pulse sequence [18].

Pulse sequence is a key concept of MRI. It directly controls the MR imaging, such as what information to be shown in the image. Pulse sequence is normally constituted by 90˚ RF pulse, 180˚ RF and some other particular angle pulse based on the application requirement. 90˚ RF pulse is the excitation pulse.

The time between the two continuous excitation pulses is called time of repeat (TR); the time interval from the excitation pulse to the MR signal measurement is called time to echo (TE). TR and TE are equipment parameters to be justified [26].

www.manaraa.com

Figure 2. 10 Time of repeat (TR) is the duration interval between two RF pulses.

The most basic pulse sequences are: partial saturation pulse sequence, saturation pulse sequence, inversion recovery pulse sequence, RF spins echo pulse sequence and gradient echo pulse sequence [31].

In the partial saturation pulse sequence and saturation pulse sequence, a sequence of 90 ˚ RF pulse is used to excite the signal.

Figure 2. 11 The partial saturation pulse sequence and saturation pulse sequence are constituted only by 90 ˚ RF pulses. The different is the TR parameter.

For partial saturation pulse sequence, the repeat time between 90 ˚ RF pulses (TR) is short, so the longitudinal magnetization (T_1 recovery) is partially recover, and the time between the 90 ˚ RF pulse and the measurement of the MR signal (TE) is minimal, immediately after the application of the 90 ˚ RF pulse, the signal is measured. In saturation recovery pulse sequence, the TR is long enough to recover all the longitudinal magnetization before the application of the next 90 ˚ RF pulse. After the 90 ˚ RF pulse, the maximum recovered signal is measured immediately. By application the partial

www.manaraa.com

saturation pulse sequence, T_1 weighted image can be generated. The image generated by application the saturation pulse sequence is called proton density weighted image.

Inversion pulse rotates the magnetization vector from the direction of the main magnetic field (the positive Z axis) to the negative direction, for example by using a 180 ˚ RF pulse before the application of the excitation pulse. The pulse sequence that uses an inversion pulse before the first excitation pulse is called inversion recovery pulse sequence. The time delay between the inversion pulse and the excitation pulse is called the inversion time (TI).

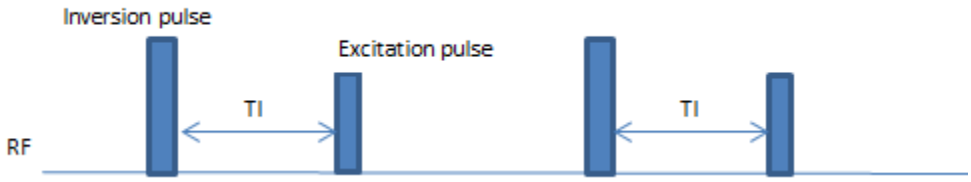

Figure 2. 12 The inversion recovery sequence.

Inversion recovery sequence begins with a 180 ˚ RF pulse. After delay time TI, the first excitation pulse 90 ˚ RF pulse is applied, then repeat this process with interval time TR.

Last but the most fundamental pulse sequence is the spin echo pulse sequence. The spin echo pulse sequence is beginning with the excitation pulse that followed with one or more refocusing pulses. The signal generate by spin echo pulse sequence is called echo. The time between excitation pulse and echo signal acquisition is echo time (TE).

www.manaraa.com

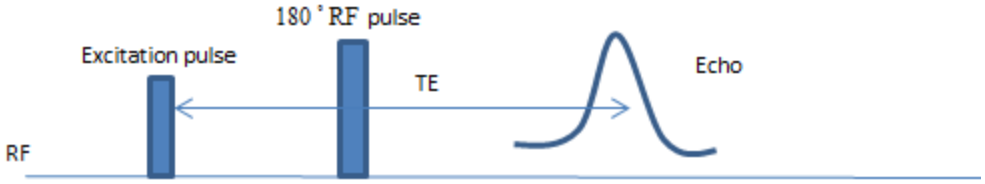

Figure 2. 13 A normal single echo Spin Echo pulse sequence. TE is interval between the excitation pulse and echo acquisition.

The spin echo pulse sequence can compensate the inhomogeneous of the external magnetic field. By control the TE and TR parameters, the spin echo pulse sequence can be used to generate T_1 weighted, T_2 weighted, and proton density weighted image.

www.manaraa.com

Chapter 3 The Earth's Field Magnetic Resonance System

Earth's Magnetic Field

The Earth's magnetic field is a dipole field which varies depending on the geographical position. According to the national geophysical data center (NGDC), in the zone of North America the magnitude is close to 50 μT. The related research shows that the homogeneity and the short time stability of the Earth's magnetic field meet the basic requirement of NMR imaging [31].

Since 1954, Earth's field NMR has been used for the demonstration of magnetic resonance principles and other geophysical research [32]. Recent research of low field NMR also demonstrated the possibility of obtaining analytical information in the absence of strong magnetic fields [33, 34]. The Earth's field magnetic resonance (EFNMR) is a special case of low field NMR. It has been applied to a broader range including multi-dimensional imaging [35, 36], high resolution spectroscopy [32, 37].

EFNMR System Components

The Earth's field magnetic resonance (EFNMR) system consists of three main hardware components: a coil probe, a digital signal processor (DSP) and a computer. The system is controlled by the computer that running data processing package Prospa. The Prospa program includes many macros. The macro provides a platform to configure the timing parameters of the signal acquisition pulse sequence. Base on the MRI principles, by

www.manaraa.com

configure the timing parameters to control the pulse sequence and complete the experiment.

Figure 3. 1 The probe used in the experiment. It consists of three sets of coil.

The coil probe consists of three set coils that slot together in a bayonet configuration. The outermost coil is coaxial solenoid, called polarizing coil. If applied with a large current, polarizing coil will produce an initial polarizing field to enhance the net nuclear magnetization of the subject sample in the probe. The middle coils are gradient coils. These coils can generate four sets magnetic field gradients. The X, Y and Z gradients are applied around the sample for spatial information encoding, the fourth gradient is for shimming. The inner coil is another coaxial solenoid, called B1 coil. B1 coil generates the pulse that both excite and detect the magnetic resonance Signals.

www.manaraa.com

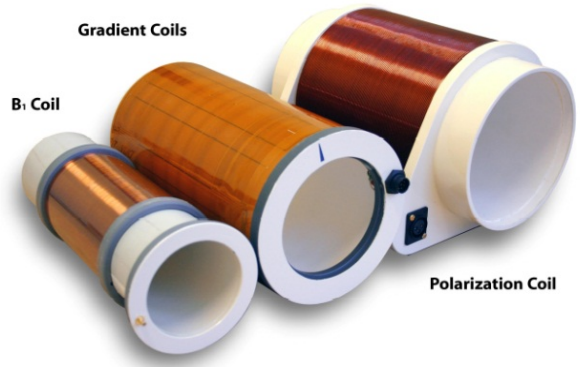

Figure 3. 2 The three sets of coils: B1 coil, Gradient Coil and Polarization Coil.

The digital signal processor (DSP) is the central control unit between the coil probe and computer. The connection between DSP and B1 coil form a LCR circuit. B1 coil frequency is set by tune the capacitance of LCR circuit.

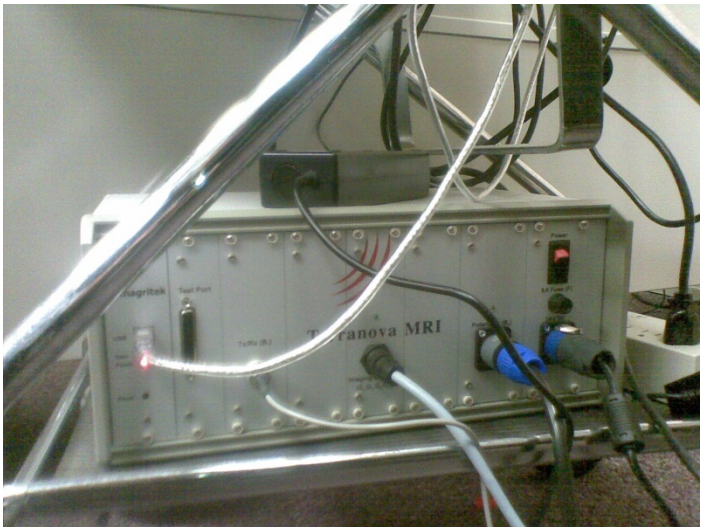

Figure 3. 3 The digital signal processor. It controls the probe.

The flowchart below describes the whole process of a regular EFNMR system experiment. The DSP is the information exchanger between the computer and the probe. The DSP receives precompiled pulse programs and parameters from the computer. After

www.manaraa.com

processing these programs, DSP will send related pulses to the coils of the probe. With the control of DSP, the probe will acquire the Magnetic Resonance signals at the appropriate time. Finally, the acquired data will be received by the computer through the DSP.

Figure 3. 4 The flow chart describes the whole working process of the EFNMR system.

EFNMR Magnetization

In the case of conventional MRI, the high field produced by the superconducting magnets is able to form a bulk net magnetization in the subject. In the EFNMR system, the Earth's magnetic field too weak to form a normal net magnetization. The approach to enhance the net magnetization is to apply another magnetic field. This magnetic field is generated by the polarization coil and called polarization pulse. It is many times greater than the Earth's magnetic field. Its direction is perpendicular to the Earth's magnetic field.

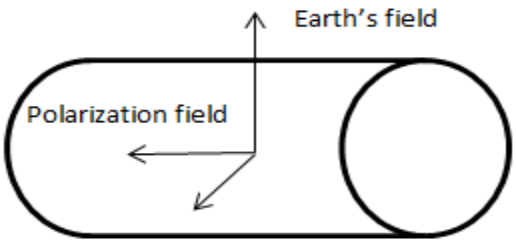

Figure 3. 5 The polarization field is applied perpendicular to the Earth's magnetic field.

www.manaraa.com

In the EFNMR system, this polarization magnetic field Bp is applied before the excitation pulse. This polarization magnetic field lasts for several spin lattice time T1. In this experiment, the polarization duration is about four or five seconds.

At the natural state, most hydrogen nuclear spins are in random distribution. With the application of the polarization magnetic field, all hydrogen nuclear spins will be oriented along the direction of the polarization magnetic field.

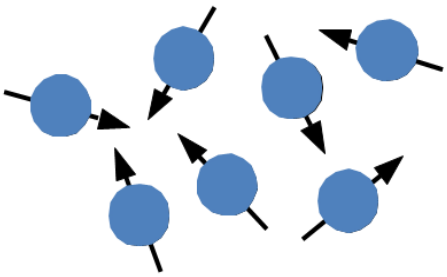

Figure 3. 6 Hydrogen nuclear spins of the sample in the nature state. They are random direction.

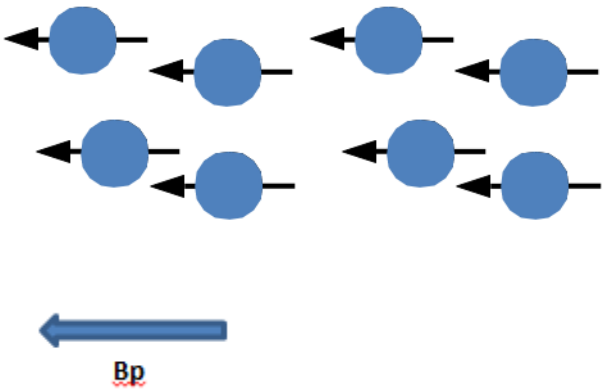

Figure 3. 7 After the application of polarization field Bp, all spins aligned along the Bp direction.

The ensemble of this re-oriented spins will form a bulk nuclear magnetization in the same direction of the polarization magnetization. After that, the current in the polarizing coil is

www.manaraa.com

switched off gradually [31]. Finally the bulk nuclear magnetization will follow the Earth's magnetic field. In the experiment, the polarization magnetic field is used to form the net nuclear magnetization and increase its magnitude for the following processing.

Excitation Pulse

Earth's magnetic field differs in location. According to the national geophysical data center (NGDC), for the location of our university (Coral Gables, Miami), the Earth's magnetic field strength is about 44.5 μT. The gyromagnetic ratio of hydrogen is 42.576 $MHz.T^{-1}$. Based on the Larmor equation (Eq.1)$\omega = \gamma * B_0$, the Larmor frequency of hydrogen in the Earth's magnetic field is calculated by:

$$\omega = \gamma * B_0 = 42.576\ MHz.T^{-1} \times 44.5\ \mu T = 1894.6\ Hz$$

In the Earth's magnetic field, the Larmor frequency is no longer in the radio frequency (RF) range but falls in audio frequency (AF) range. The corresponding excitation pulse generated by the B1 coil is not RF pulse but an ultralow frequency (ULF) pulse.

In the Earth's magnetic field, the Larmor frequency of hydrogen nuclei is about 1.90 kHz. Surround electromagnetic noise can easily influence this ultralow frequency signal and the Earth's field homogeneity. In order to reduce the external interference and improve the field homogeneity, we design a wooden stand for the EFNMR probe to keep it few meters away from the floor and the other electric source.

www.manaraa.com

Figure 3. 8 The wooden stand that supports the probe.

Pulse Sequence

Pulse sequence plays the key role in magnetic resonance imaging (MRI). The main function of pulse sequence is to manipulate the magnetization in order to generate the desired magnetic resonance (MR) signals [31].

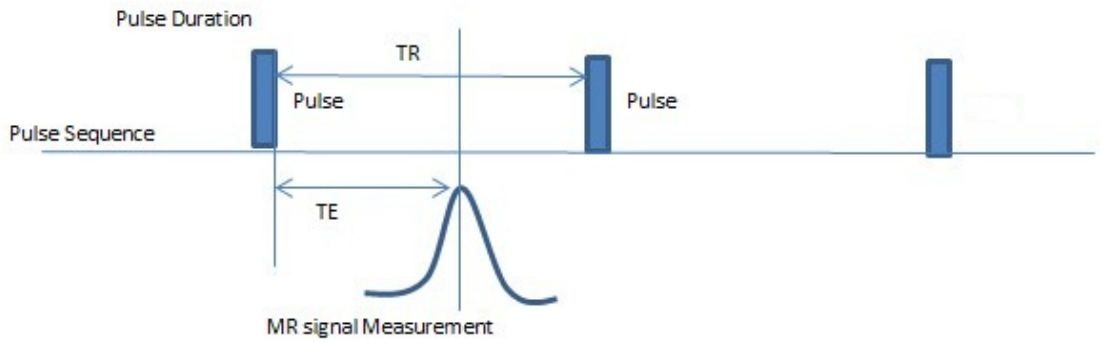

Figure 3. 9 In the EFNMR experiment, configure these timing parameters to control the pulse sequences. Timing parameters include: pulse duration, TR and TE. Pulse duration is the time that pulse is applied. TR is

www.manaraa.com

the time interval between two successive pulses. TEis the time interval between the excitation pulse and the Magnetic Resonance (MR) signal measurement.

In this EFNMR experiment, all pulses are generated by the B1 coil and polarization coil. The control of pulse sequences is via the configuration of these timing parameters: pulse duration, TR and TE. For example, 90˚ pulse and 180˚ pulse can be generated by configure pulse duration.

From the perspective of pulse sequence, the MRI experiment process in the Earth's magnetic field is as below figure. The direction of the Earth's magnetic field is along the Z axis.

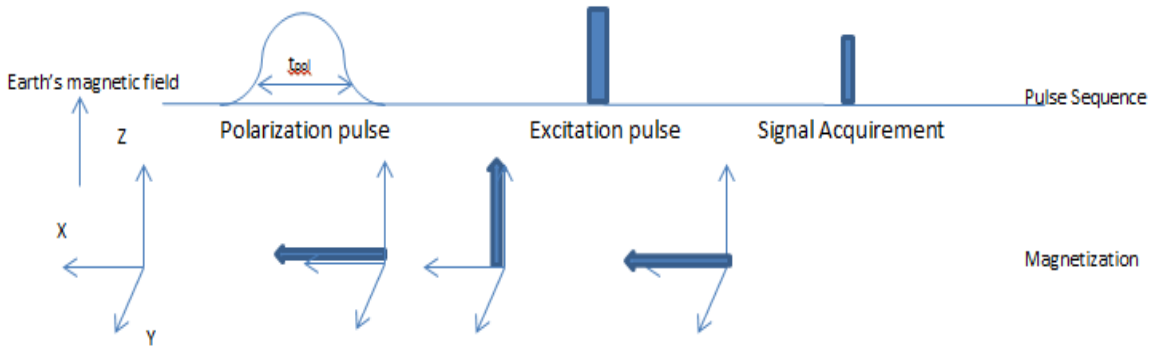

Figure 3. 10 The pulse sequence used in Earth's field experiment to acquire a signal. The second floor shows the evolvement of the magnetization direction.

At first, a polarization pulse produced by the polarization coil is applied along the X axis with duration t_{pol} to generate a bulk nuclear magnetization in the sample. Afterwards, this nuclear magnetization begins to precess along the Earth's magnetic field and direct to the Z axis. With particular time delay, the excitation pulse generated by the B1 coil is implemented. This excitation pulse is tuned to the precession frequency of the sample

www.manaraa.com

magnetization. The magnetization is flipped down to the X-Y plane by the excitation pulse. The flip angle is controlled by the duration of the excitation pulse. Then excitation pulse is turned off. With a short delay, the magnetization component in the X-Y plane will be detected. This is considered as the magnetization resonance (MR) signal. The signal detection process is also completed by the B1 coil.

www.manaraa.com

Chapter 4 EFNMR Experiment

The low field coil probe was used to cast the Magnetic Resonance Imaging (MRI) teaching demonstration in the lab environment. This demo includes several experiments: magnetic resonance (MR) signal collecting, the measurement of relaxation parameters and the simulation of relaxation time weighted images.

Experimental Samples

As it is the hydrogen magnetic resonance (MR) signal that is measured in MRI [38], the ideal sample is tap water. Besides, another sample with different relaxation property is also prepared: the copper sulfate solution. Copper ions are paramagnetic ions. The paramagnetic ions can increase the relaxation rate of the water so that shorten the relaxation time of the water molecule [39] [40]. These two samples were used to simulate relaxation time weighted image.

Parameters Initialization

Firstly, the polarization duration of 4 seconds was applied to get the enhanced nuclear magnetization along the earth's direction.

Secondly, set the frequency of $B1$ coil equals the Larmor frequency of the hydrogen spin in the laboratory environment. An inaccurate B1 frequency can significantly decrease the signal.

The Prospa program provides macro to measure the accurate resonance frequency of B1 coil. At first, the Analyse Coil macro from the Prospa program provides the curve of

www.manaraa.com

resonance frequency versus capacitance and the B1 coil characteristics: B1 coil capacitance = (4.50 ± 0.02) nF; B1 coil inductance = (0.3755 ± 0.0004) H.

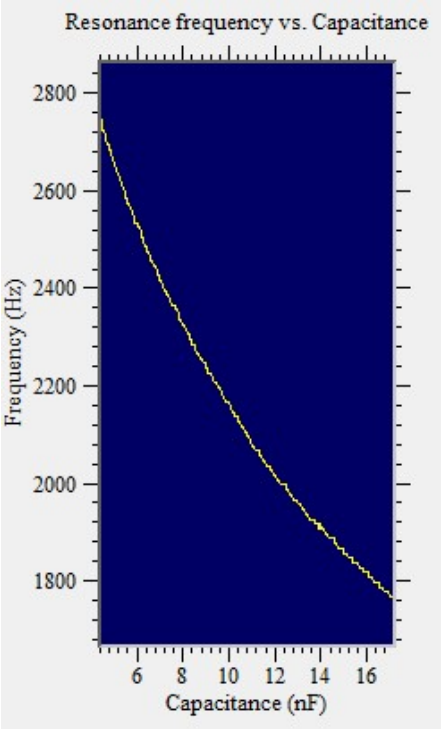

Figure 4. 1 The curve of resonance frequency versus capacitance

Then run the Autotune macro and filled in the B1 coil characteristics, as the figure follow.

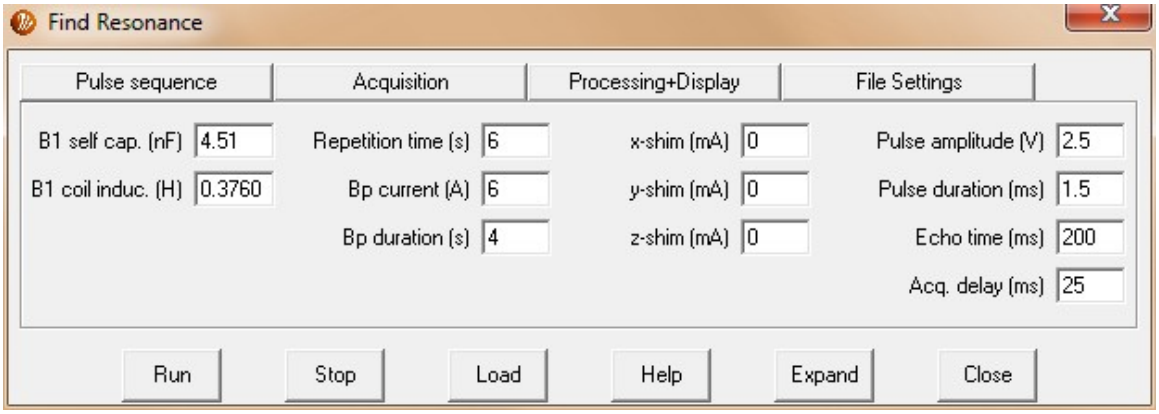

Figure 4. 2 Autotune experiment

www.manaraa.com

During the Autotune experiment a series of spin echo pulse sequence with different B1 pulse frequencies are applied to the sample. The variable B1 pulse frequencies are realized by tuning the capacitance. Every capacitance value has a corresponding time domain signal result. A two dimensional (2D) matrix is used to store these time domain signals. Each row stands for the corresponding capacitance value, as figure below.

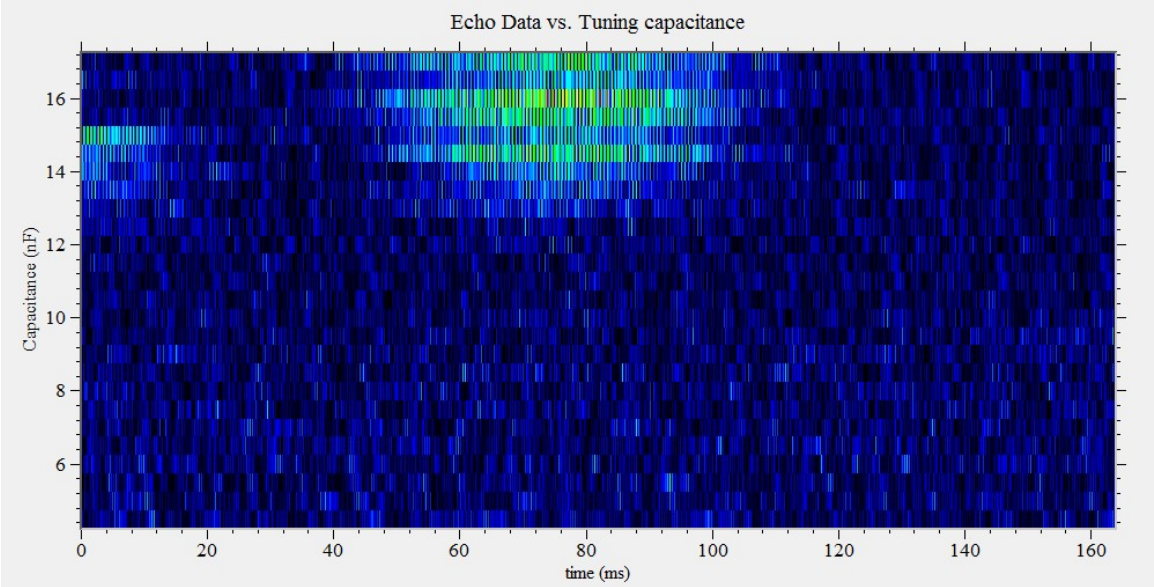

Figure 4. 3 The 2D figure of the Echo Signal versus Capacitance

The principle is only when B1 pulse frequency equals to the Larmor frequency of hydrogen spin, echo signal is produced. In the above figure, the echo signal is shown as the colorful region. From the figure, the row value of the colorful region is the resonance capacitance of B1 coil, which is 15.5 nF. From the curve of resonance frequency versus capacitance get the resonance frequency of B1 is 1835 Hz.

In this system B1 coil is used to both excite and collect the magnetic resonance signal. The excitation pulse produced by the B1 coil flips the nuclear magnetization with a flip

www.manaraa.com

angle α to the transverse plane. The flip angle is defined in (Eq.2) $\alpha = \gamma * B1 * \tau$. The flip angle is related to the pulse amplitude (B1) and duration (τ). By configuring the B1 coil transmit gain and B1 pulse duration to set the flip angle to get 90˚ pulse and 180˚ pulse.

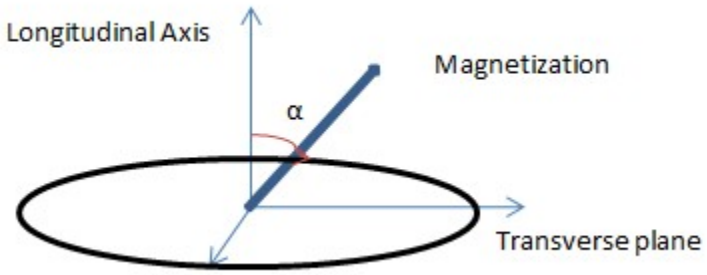

Figure 4. 4 The excitation pulse produced by the B1 coil flips the nuclear magnetization with a flip angle α to the transverse plane.

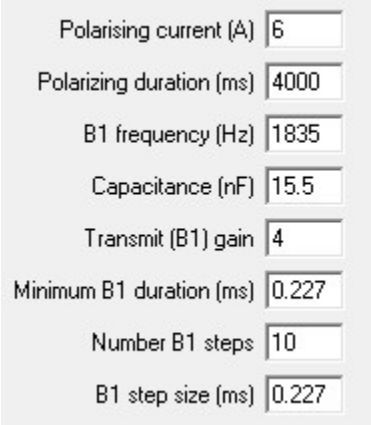

Figure 4. 5 The parameter set of B1 Duration experiment.

Thirdly, calibrate the tip angle to get 90˚ pulse and 180˚ pulse. Run the B1 duration macro from the Prospa program and filled in the data set as above figure. In this experiment, a series B1 pulses with constant transmit gain but variable pulse duration were applied to

www.manaraa.com

the water sample. The resulting transverse magnetizations were detected by the B1 coil. B1 transmit gain was set to 4. The duration began with 0.227 ms and twice in the next step till to 2.27ms. The table below is the result of pulse duration and the corresponding transverse magnetization.

Table 1 The experiment result of different pulse duration and the corresponding transverse magnetization. All the result transverse magnetization is recorded in the second row.

Duration	0.227	0.454	0.681	0.908	1.135	1.362	1.589	1.816	2.043	2.27
Magnetization	85.5	90.2	80.5	76	8.9	48.8	84.7	83.1	49.9	58.3

Using the B1 duration parameters as X axis and the corresponding transverse magnetization values as Y axis, the relationship between B1 duration and transverse magnetization was plot as below figure. The transverse plane magnetization component is measured as the magnetic resonance signal. With a 90˚ flip angle, the nuclear magnetization is fully tipped down in the transverse plane to produce the maximum signal. With an 180˚ flip angle, the magnetization is tipped to the opposite direction with no signal detected.

www.manaraa.com

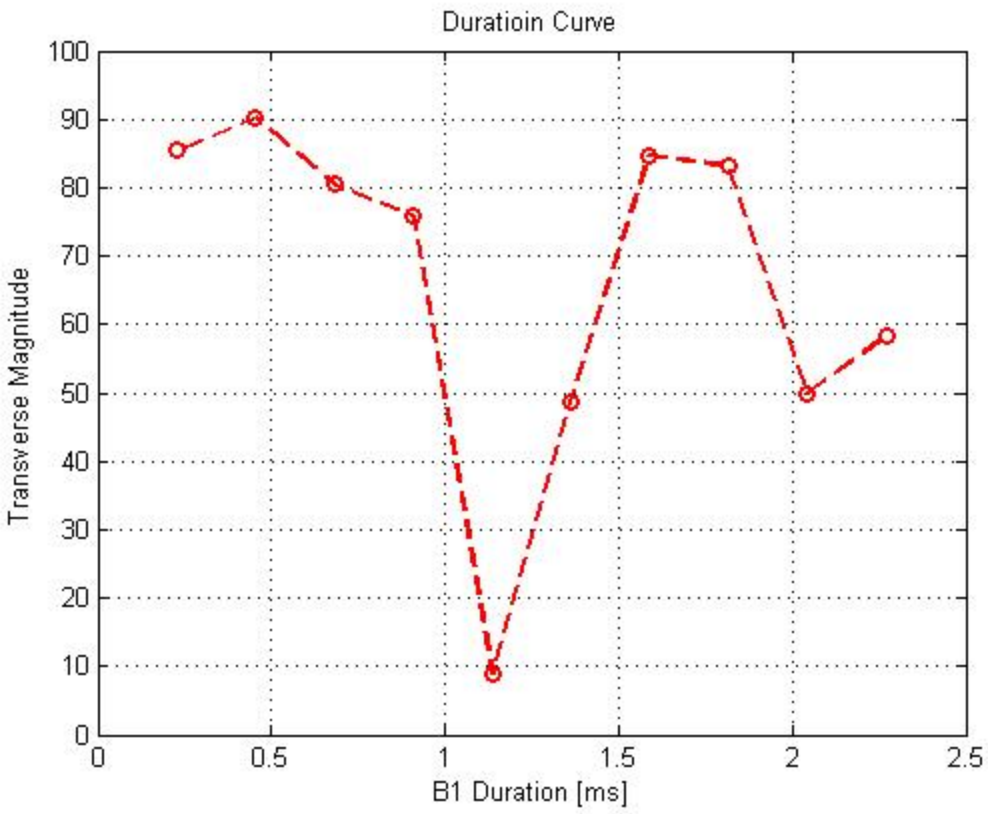

Figure 4. 6 This plot is the transverse magnetization VS the B1 Duration.

In the figure, the first maximum magnetization is corresponding the 90˚ pulse duration, which is 0.454 ms. The followed minimum magnetization is corresponding to the 180˚ pulse duration, which is 1.135 ms.

According to the flip angle equation (Eq.2), if B1 pulse magnitude increase, the corresponding duration will reduce. In the experiment, if the B1 transmit gain reduced to 2.5, the duration of 90˚ pulse is 0.868 ms and 180˚ pulse duration is 1.953 ms.

www.manaraa.com

Magnetic Resonance (MR) Signal Collecting

In this experiment, the water sample was used to collect the two basic type MR signals: free induction decay (FID) signal and spin echo signal.

Free induction decay (FID) signal is the observed result from the hydrogen spin system after a transient 90˚ pulse. It shows the decay process of magnetization in the transverse plane.

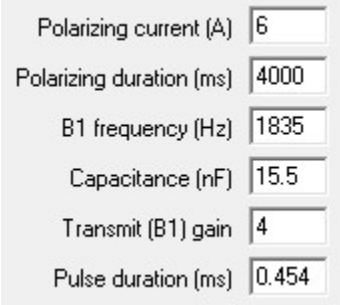

Figure 4. 7 The parameter set of FID collection experiment.

The Pulse and Collect macro was chosen to perform the free induction decay (FID) collection experiment. The parameter set of this experiment is as above figure. With transmit gain was set to 4 and pulse duration equals to 0.454 ms, the tip angle was set to 90 degree. This free induction decay (FID) collection experiment is carried out using the basic polarizing pulse sequence. This pulse sequence is a series repeat of polarizing pulse and 90˚ excitation pulse. The result FID signal is shown below.

www.manaraa.com

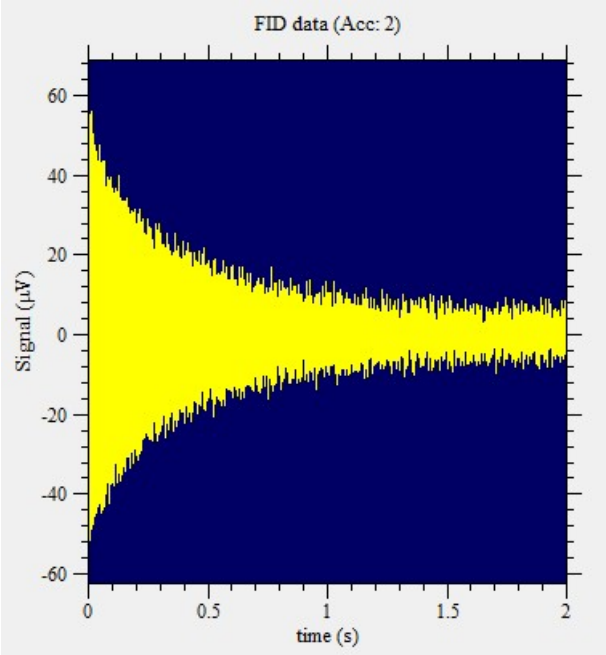

Figure 4. 8 The free induction decay (FID) signal get in the project. It shows the decay process of the magnetization in the transverse plane.

To get the echo signal, both 90˚ pulse and 180˚ pulse are implemented. Chosen the Spin Echo macro from the Prospa program. The parameter set was as below figure.

Polarizing current (A)	6
Polarizing duration (ms)	4000
B1 frequency (Hz)	1835
Capacitance (nF)	15.5
Transmit (B1) gain	4
90 pulse duration (ms)	0.454
180 pulse duration (ms)	1.135

Figure 4. 9 Spin echo pulse sequence parameter set.

This experiment used a spin echo pulse sequence which includes a 90˚ pulse and a refocus 180˚ pulse. This 180˚ pulse refocuses the magnetization in the transverse plane,

www.manaraa.com

which lead to a re-growth process of signal. This process results in an echo signal. Echo signal collected by the application of spin echo pulse sequence is shown below.

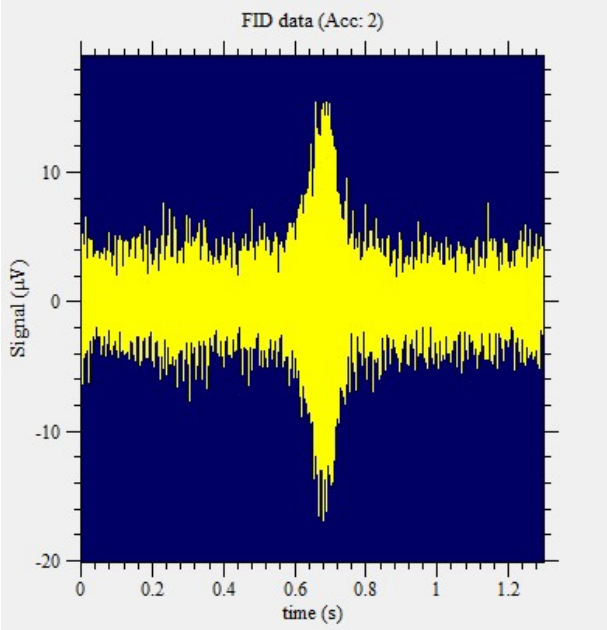

Figure 4. 10 The echo signal. It shows the regrowth process after the application of refocus pulse.

Measurements of Relaxation times

The spin-lattice relaxation time T_1 and the spin-spin relaxation time T_2 are characteristic parameters of the sample. They are the primary source of inherent contrast of tissues in MRI [41].

Spin relaxation time parameters are very important material property. They are wildly used in medical research such as human blood study [42], osteoarthritis study [43] and neurological diseases study [39] and other biological field [44].

In this experiment, we measured T_1 and T_2 values of two different materials: water and copper sulfate solution.

www.manaraa.com

The Bloch equation [6] is the theory foundation for estimating the values of T_1 and T_2. It quantitatively describes the time dependent evolution of the nuclear magnetization after the application of the magnetic field B1 [45]. For MRI, the Bloch equation is as the below form [24]:

$$\frac{dM}{dt} = \gamma M \times B - \frac{M_x i + M_y j}{T_2} - \frac{M_z - M_0}{T_1} \times k \qquad \text{Eq. 4}$$

Where, γ is the gyromagnetic ratio; M is the nuclear magnetization; B is the applied magnetic field; T_1 and T_2 are relaxation time parameters; $M_x i + M_y j$ is the transverse magnetization; $M_z \times k$ is the longitudinal magnetization; $M_o \times k$ is the equilibrium nuclear magnetization.

The solution of the Bloch equation describes the relaxation process of both the longitudinal magnetization component and the transverse magnetization component [18].

$$M_z(t) = M_z(0)\exp\left(-\frac{t}{T_1}\right) + M_0[1 - \exp(-t/T_1)] \qquad \text{Eq. 5}$$

$$M_{xy} = M_{xy}(0)\exp(-t/T_2) \qquad \text{Eq. 6}$$

Eq.5 indicates the relaxation process of the longitudinal magnetization component M_z. Eq.6 indicates the relaxation process of the transverse magnetization component M_{xy}. In the project, the above two equations are used to estimate the relaxation time value.

www.manaraa.com

T_1 Measurement

In order to get the nuclear magnetization in the Earth's magnetic field, a polarization magnetic field M_p will be applied for a particular duration τ_p. From the Bloch equation, we can get the relationship between the longitudinal magnetization M_z and polarization duration τ_p.

$$M_z(t) = M_p[1 - exp(-\tau_p / T_1)] \qquad \text{Eq. 7}$$

To measure the longitudinal relaxation parameter, chosen the T_1 B_p macro, the parameter set is as figure blow.

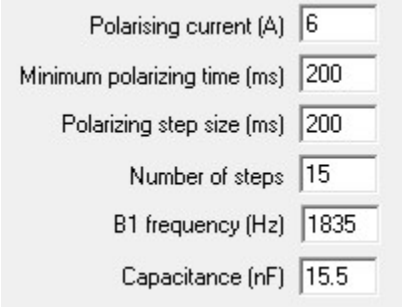

Figure 4. 11 The parameter set for T_1 measurement.

In this experiment, the pulse sequence utilized is:

(Polarization pulse – 90˚ Pulse – signal acquire)

This pulse sequence is composed by a polarization pulse with variable duration and a 90˚ pulse. This pulse sequence was repeated with the gradually increasing duration τ_p. The corresponding signal amplitude was record. We set its range from 200 ms to 3000 ms, the

www.manaraa.com

increment is 200 ms. The data record for both water and copper sulfate shown in the below table:

Table 2 This table shows the resulting magnetization amplitude VS polarization duration. The left column is the result for water. The right column is the result for copper sulfate solution.

Water		Copper Sulfate (660mM)	
Duration (ms)	Amplitude (uV)	Delay (ms)	Amplitude (uV)
200	6.7	200	14.0
400	11.8	400	22.9
600	16.3	600	29.8
800	20.5	800	35.1
1000	23.5	1000	40.6
1200	27.4	1200	43.6
1400	30.7	1400	46.6
1600	34.4	1600	49.0
1800	36.3	1800	50.8
2000	40.0	2000	52.2
2200	40.7	2200	54.1
2400	44.9	2400	54.6
2600	47.0	2600	55.8
2800	48.5	2800	58.3
3000	50.6	3000	56.9

From the data of the above table, the Polynomial interpolation method is utilized to fit the T_1 curves of both water and copper sulfate solution. The longitudinal relaxation time parameters were obtained. The values of T_1 is 2.5 s for water and 0.86 s for copper sulfate. The copper ion indeed decreases the relaxation time.

www.manaraa.com

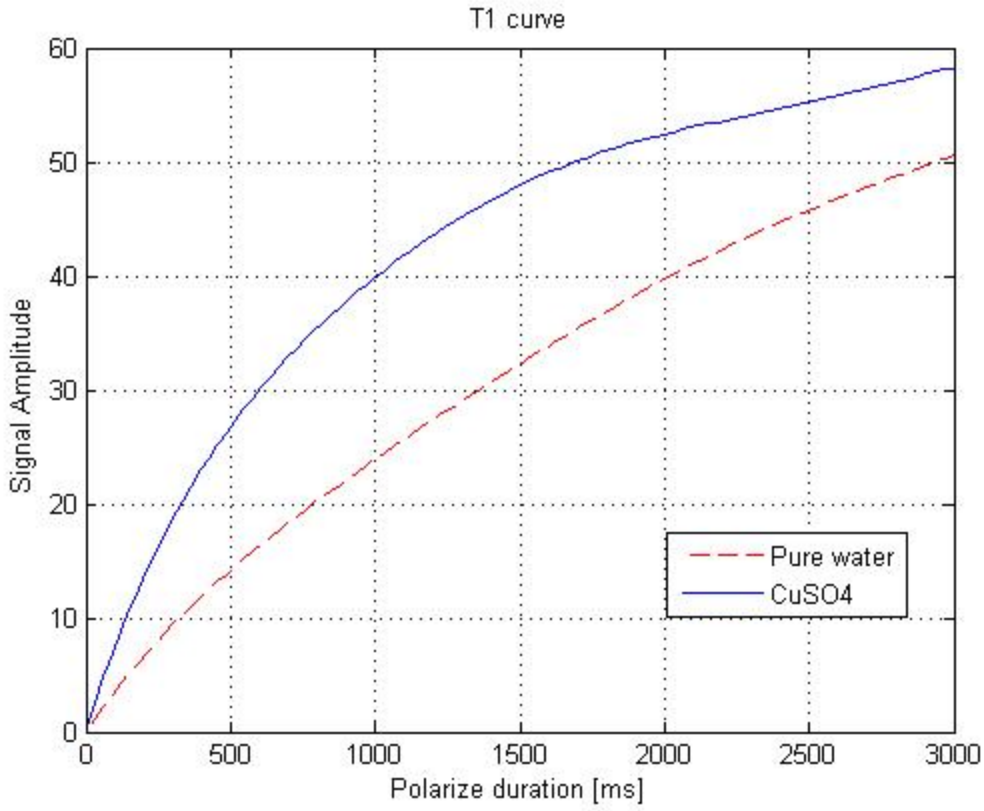

Figure 4. 12 The plot of T_1 curves. The red line is water and the blue line is copper sulfate solution.

T_2 Measurement

To measure the transverse relaxation parameter, chosen the T_2 macro, the parameter set is as figure blow.

Polarizing current (A)	6	90 pulse duration (ms)	0.454
Polarizing duration (ms)	4000	180 pulse duration (ms)	1.135
B1 frequency (Hz)	1835	Minimum echo time (ms)	100
Capacitance (nF)	15.5	Echo time step (ms)	100
Transmit (B1) gain	4	Number of steps	10

Figure 4. 13 The parameter set of spin echo pulse sequence for T_2 measurement.

www.manaraa.com

For T_2 measurement, the spin echo pulse sequence is used.

(Polarization pulse – 90 pulse – 180 pulse - signal acquire)

With spin echo pulse sequence, we can get echo signal. We repeated the spin echo pulse sequence several times with variable echo time τ_E and recorded the corresponding echo signal magnitude. The echo time doubles for every repeat. The echo time ranged from 200 ms to 2000 ms.

The relationship between the echo signal and echo time is shown in the follow equation:

$$E(t) = E(0)\exp(-\tau_E/T_2) \quad \text{Eq. 8}$$

The data record for both water and copper sulfate shown in the below table:

Table 3 This table shows the resulting echo signal amplitude of the different echo time. The left column is the data result of water. The right column is the data result of the copper sulfate solution.

Water		Copper Sulfate (660mM)	
echo time(ms)	E	echo time(ms)	E
200	40.5	200	41.1
400	35.6	400	29.6
600	33.4	600	22.1
800	30.1	800	17.6
1000	26.4	1000	13.2
1200	24.7	1200	10.2
1400	21.8	1400	8.3
1600	19.4	1600	4.6
1800	18.1	1800	4
2000	16.4	2000	3.3

www.manaraa.com

From the data of the above table, the Polynomial interpolation method is utilized to fit the T_2 curves of both water and copper sulfate solution. The transverse relaxation time parameters were obtained. The values of T_2 is 2 s for water and 0.8 s for copper sulfate. The copper ion indeed decreases the relaxation time.

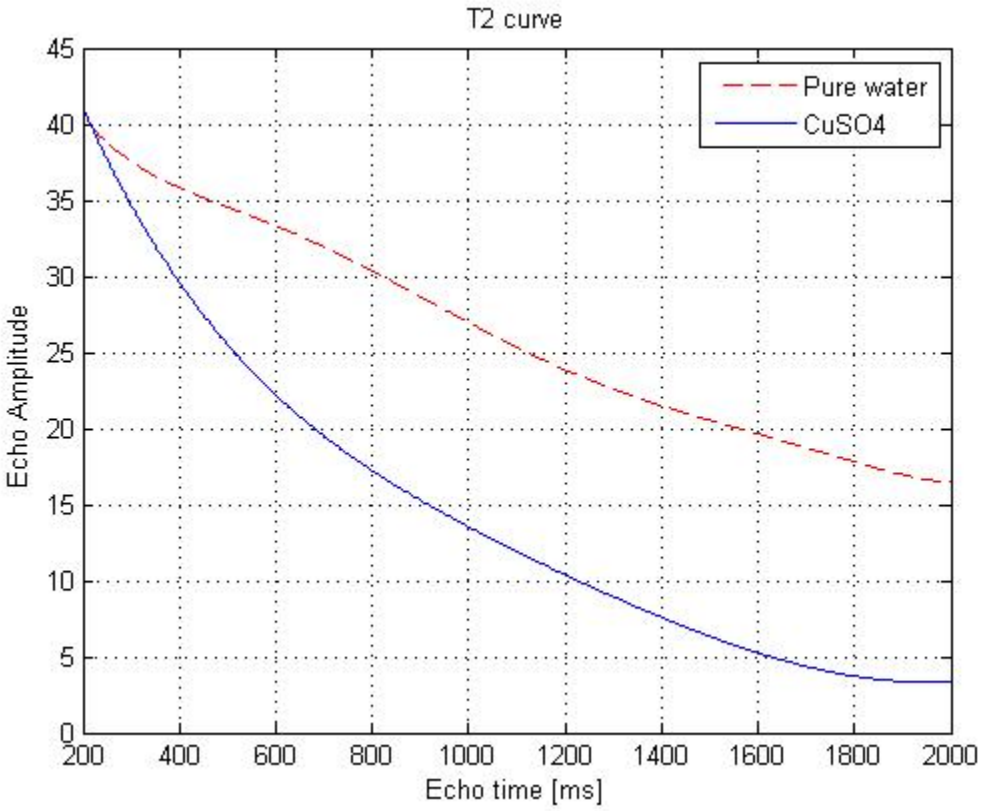

Figure 4. 14 The plot of T_2 curves. The red line is water and the blue line is copper sulfate solution.

Relaxation Time Weighted Effect Image

This experiment is to simulate the contrast mechanism in magnetic resonance imaging (MRI) in the Earth's magnetic field with the low field coil probe.

www.manaraa.com

Image contrast between two adjacent regions in an image is defined in terms of image intensity differences [18]. Image intensity is proportional to the nuclear magnetization. From the Bloch equation (Eq.4), the nuclear magnetization is a multi-parameter function. However, with special configured data acquisition tool – pulse sequence, we can control which parameter effect is dominant. If it is T_1 property dominate called T_1 weighted image. This material characteristic parameters weighted image is the basic contrast mechanism in magnetic resonance imaging [46].

The detected signal is proportional to the nuclear magnetization. In this experiment, the amplitude of the nuclear magnetization is proportional to the polarization pulse duration. The magnetization difference between the two samples produced by the polarization pulse duration is due to the different T_1 properties. The polarization pulse duration can be utilized to get the T_1 effect.

www.manaraa.com

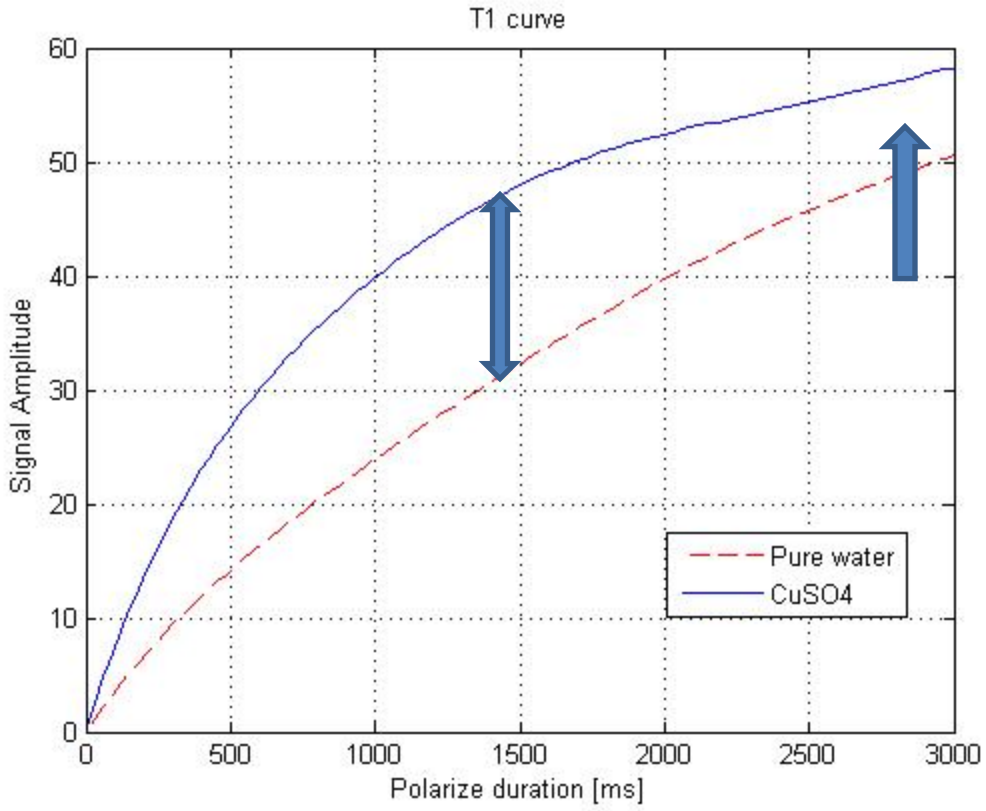

Figure 4. 15 When polarization duration smaller than 1500 ms will produce the most significance difference of the signal amplitude. When polarize duration is more than 3000 ms, it tends to have no difference.

From the T_1 curve, the tendency is that when polarization duration smaller than 1500 ms the most significance difference of the signal amplitude will be produced. When polarize duration is growing bigger than 3000 ms, it tends to have no difference. A long polarization duration value, such as more than 3000 ms, can be used to eliminate T_1 effect.

The signal difference produced by the echo time is due to the different T_2 properties. Echo time is utilized to get the T_2 effect. Image different due to T_2 effect is referred as T_2 weighted image.

www.manaraa.com

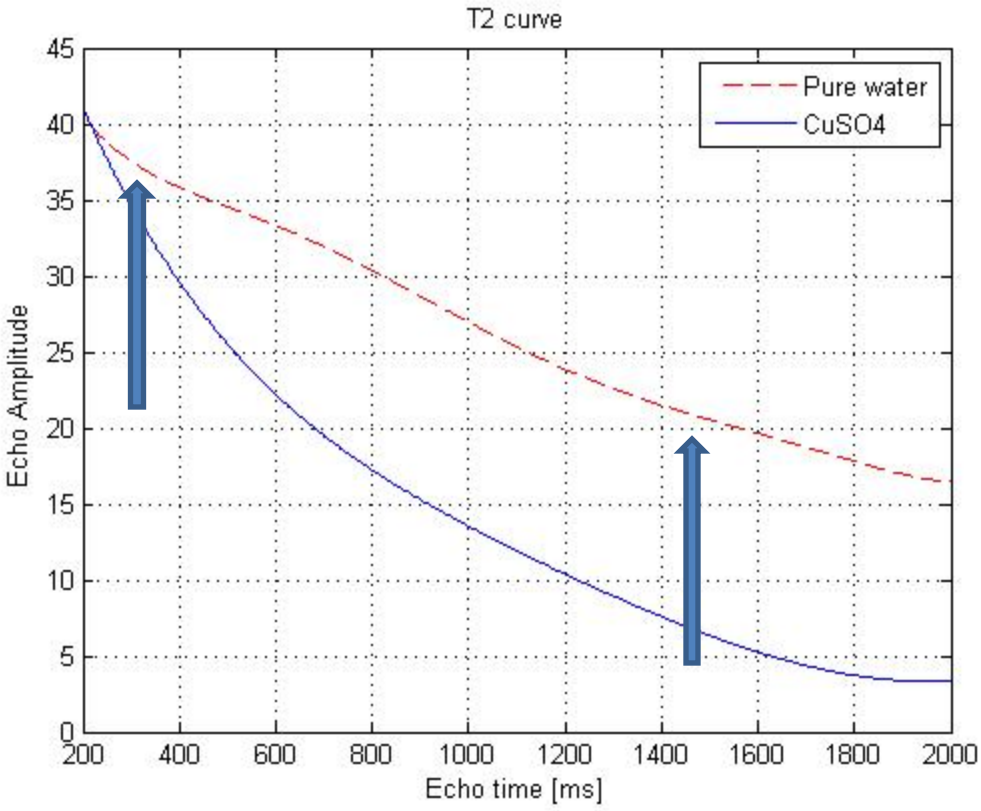

Figure 4. 16 The smaller the echo time, the less difference. The echo difference between the two samples is proportional to the echo time. With the increasing of echo time, the difference is increase too.

From the T_2 curve, the signal different evolve tendency is that: the smaller the echo time, the less difference. Basically, a small echo time value can be used to reduce the T_2 effect. Bigger echo time get the T_2 effect.

In conclusion, the method to generate relaxation time weighted effect is by manipulation polarization pulse duration and echo time of the pulse sequence.

In this experiment, Gradient Echo Imaging macro is chosen from the Prospa program. A basic gradient echo imaging pulse sequence was used to get T_1 and T_2 weighted image.

www.manaraa.com

To get a T_1 weighted image, polarization pulse duration is set to 1300 ms to enhance the T_1 effect and echo time is 210 ms to eliminate the T_2 effect. The data set is as follow figure.

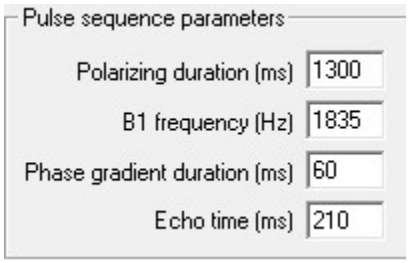

Figure 4. 17 Parameter set for T_1 weighted image.

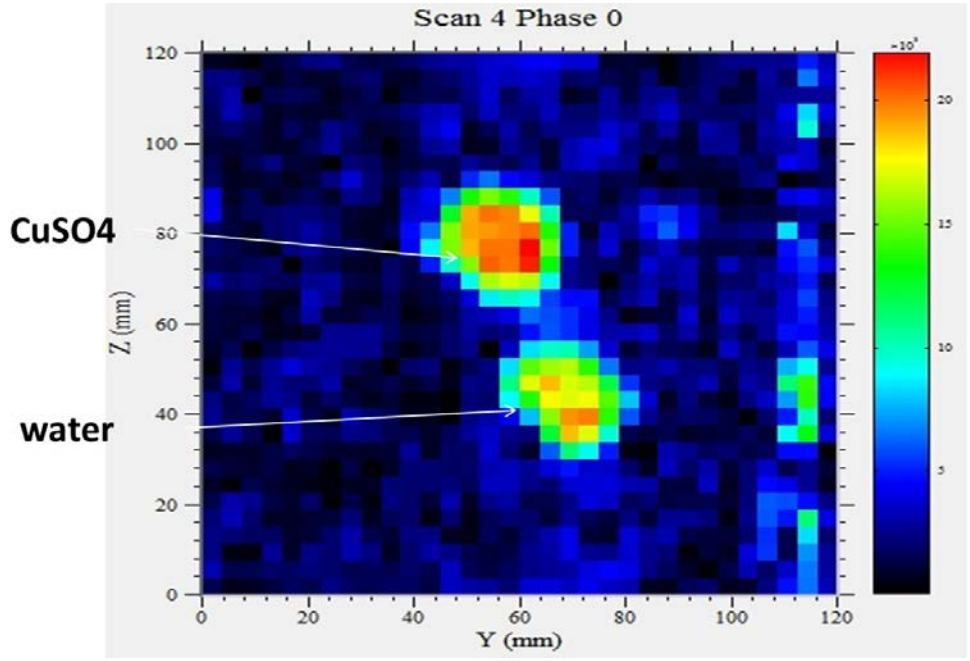

Figure 4. 18 This is the image result to simulate the T_1 weighted effect image. The FOV of this image is 120*120 mm. Polarization duration is 1300 ms, echo time is 210 ms. In this image, the copper sulfate is brighter than the water.

www.manaraa.com

To get a T_2 weighted image, polarization pulse duration is set to 3000 ms to eliminate the T_1 effect, and echo time is 320 ms to enhance the T_2 effect. The data set is as follow figure.

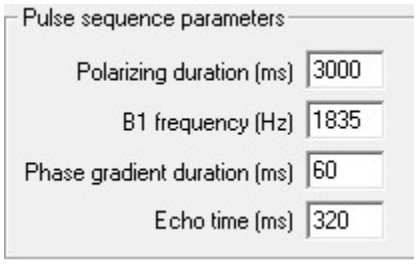

Figure 4. 19 Parameter set for T_2 weighted image.

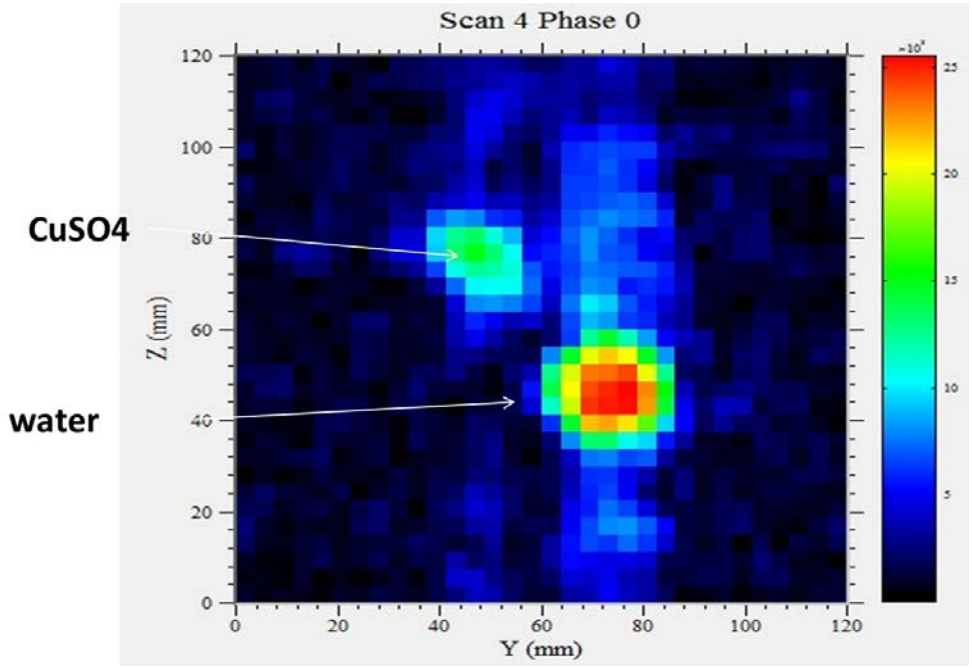

Figure 4. 20 This is the image result to simulate the T_2 weighted effect image. The FOV of this image is 120*120 mm. Polarization duration is 3000 ms, echo time is 320 ms. In this image, the water is brighter than the copper sulfate.

www.manaraa.com

Compare the two figures, in T_1 weighted image, copper sulfate is brighter than the water, in T_2 weighted image, the situation is reversed. Basically, this is the main function of relaxation weighted image in clinical field, based on the tissue specific relaxation properties, by manipulate the timing parameters of the imaging pulse sequence, specialist can get the desired image to have particular tissue enhanced display.

www.manaraa.com

Chapter 5 Graphical User Interface Tutorial

This part is to build a simulation platform to mimic MRI signal acquisition and reconstruction process by graphical user interface. The simulation is based on a noiseless condition. A 2D matrix data set serves the phantom. Data value is then proportional to the simulate proton density. The GUI-based simulation provides students online demonstrations of combined resonance signal, K-space construction, and FFT used to decompose signal from frequency domain back to spatial domain in an interactive fashion.

Magnetic Resonance Signal Tutorial

The first GUI window is about magnetic resonance (MR) signal simulation.

A three by three matrix is configured to simulate the two dimension distribution of hydrogen spins in the particular cross sectional anatomy plane. The density of hydrogen spins is directly proportional to the element value in the matrix. An ideal noiseless condition is assumed in the tutorial, the relaxation process is not considered. Each element of the matrix produces a MR signal. The combination of these signals is the final MR signal that is detected [47]. Fourier transform is applied on this combined MR signal to recover the individual signals [48]. Gradient magnetic field is used to spatial encoding these magnetic resonance signals [20]. The Larmor frequency of these magnetic resonance signals will be different according to their location [22]. This spatial encoding process will be repeated many times to get several signals. These signals fill up the data space, also referred as K-space [19]. Fast Fourier transform (FFT) approach is used to reconstruct the MR image [49].

www.manaraa.com

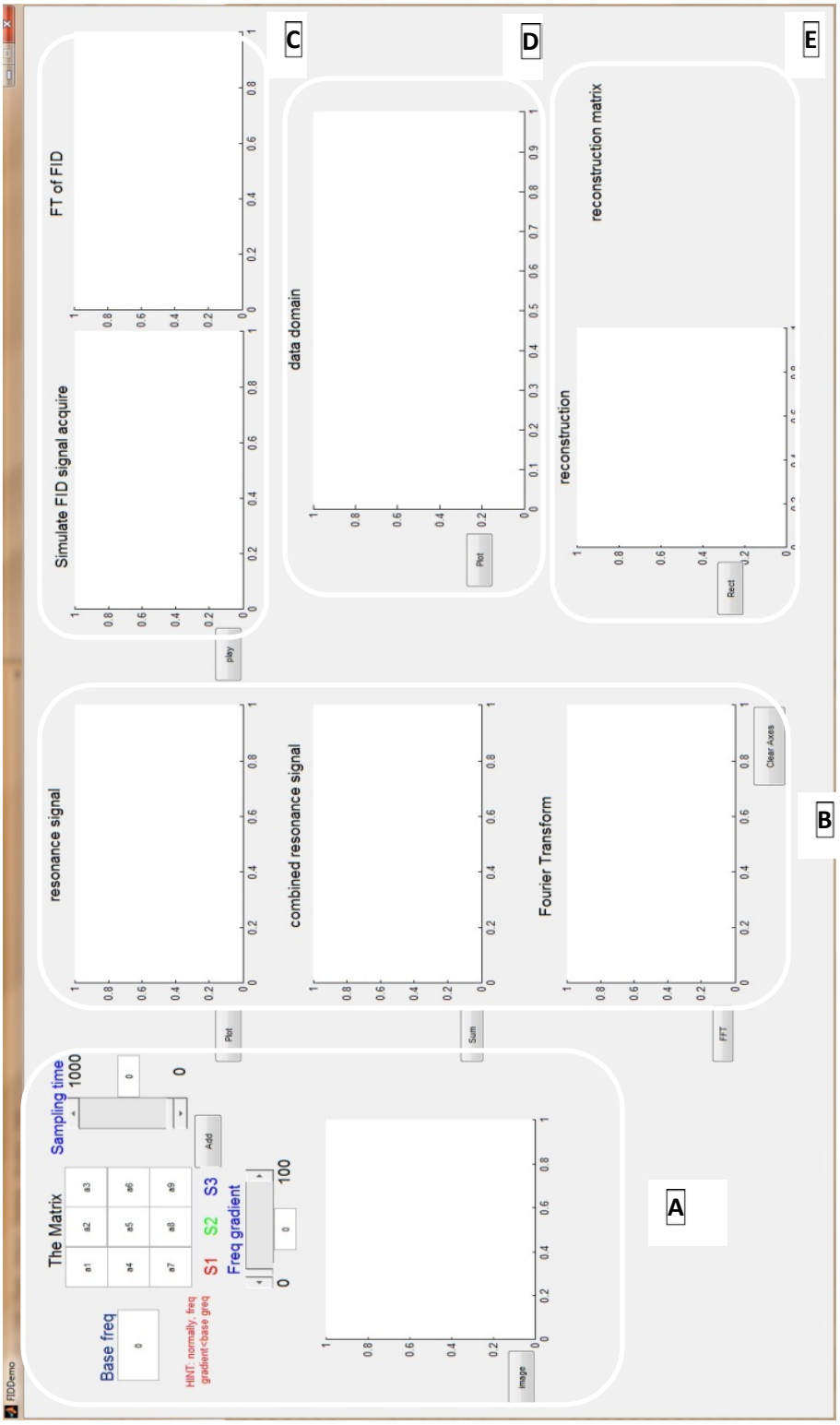

Figure 5. 1 The Magnetic Resonance Signal Tutorial. All simulation in this tutorial is based on the 3by3 matrix. From the perspective of function, this tutorial GUI is separated into five parts.

www.manaraa.com

From the perspective of function, this GUI tutorial is separated into five parts. Part A shows the linear magnetic field gradient (Eq.9). With the application of field gradient (G) along the matrix, every column will have different Larmor frequency.

$$\omega = \gamma(B_0 + G) = \omega_0 + \omega_G \qquad \text{Eq. 9}$$

In this tutorial, user can set the base frequency (ω_0) of the central column and the frequency gradient (ω_G) to simulate the effect of field gradient. Based on the matrix the user set, the corresponding grayscale image is shown.

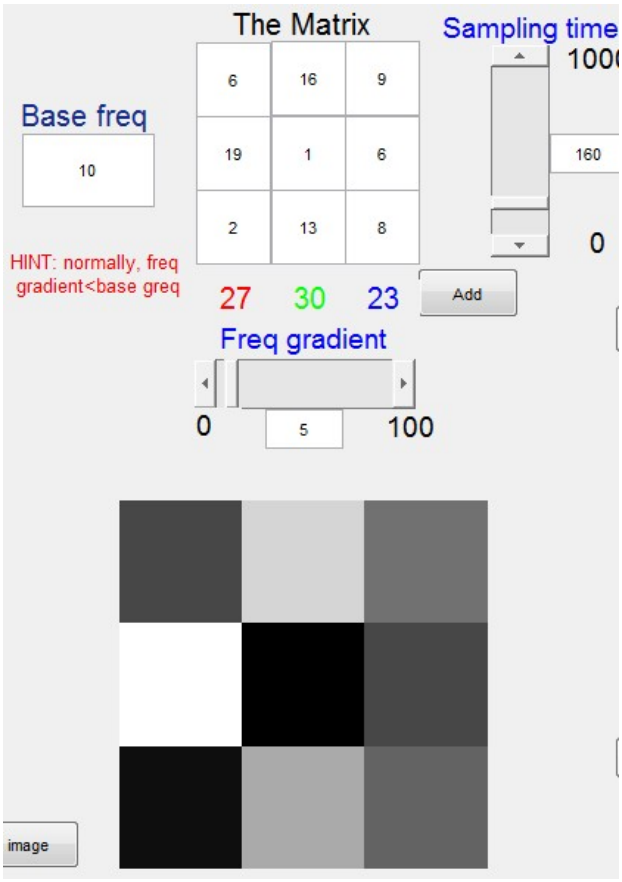

Figure 5. 2 This is Part A of the GUI tutorial. User can set the elements value of the matrix and other parameters: base frequency, frequency gradient, sampling time. User should notice that the base frequency should larger than the frequency gradient. The grayscale image is also shown below.

www.manaraa.com

Part B simulates the individual signal and the combined signal. Also, the effect of Fourier transform is shown in this part.

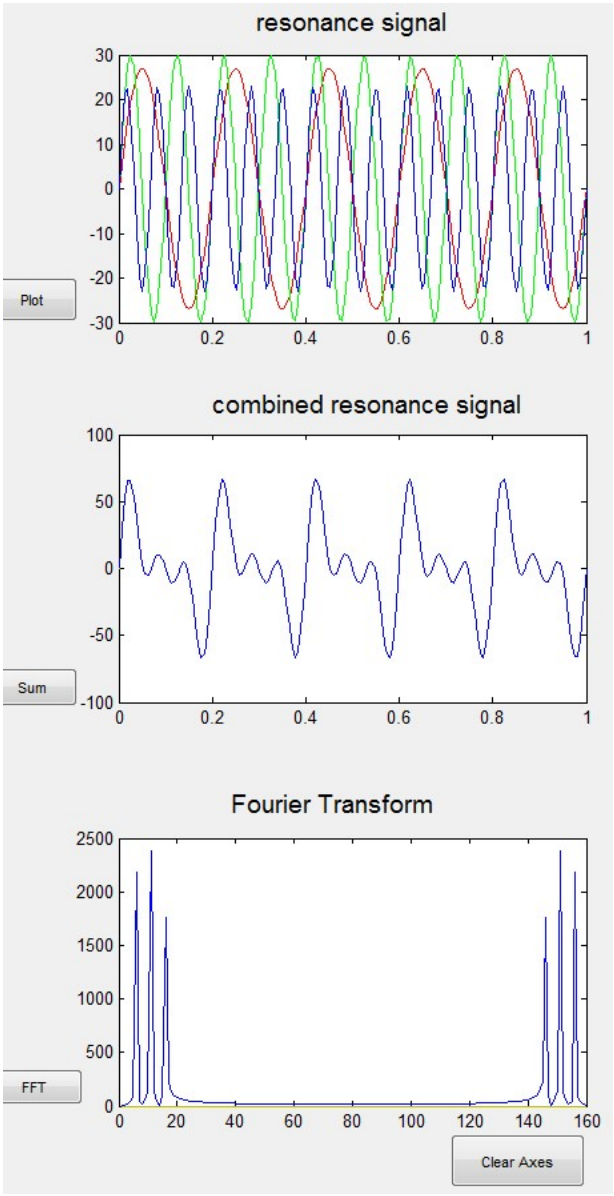

Figure 5. 3 This is part B of the GUI tutorial. The simulated magnetic resonance signals and their combination is shown. Fourier transform is applied to discompose the combined magnetic resonance signal.

www.manaraa.com

In part B, the first plot is the sampled signal of each column. The magnetic resonance signal of every point is shown in the follow equation:

$$signal(x,y) = \rho(x,y) * \mathrm{e}^{-i\gamma(B_0+G)t} \qquad \text{Eq. 10}$$

$\rho(x,y)$ stands for the spin density of the particular location (x, y). We assume spin density of the particular location (x, y) is proportional to the corresponding pixel value. G is the magnetic field gradient. The equation $\mathrm{e}^{-i\gamma(B_0+G)t}$ simulates the frequency encoding process. Every column will have different Larmor frequency.

The second plot is the combined signal of the whole matrix. The mathematic expression of the combined signal is as the follow equation:

$$combined\ signal = \iint signal(x,y)\, d_x d_y \qquad \text{Eq. 11}$$

$$= \iint \rho(x,y) * \mathrm{e}^{-i\gamma(B_0+G)t}\ d_x d_y$$

Basically, the combined signal is the sum of the signals from every elements of the matrix.

At the third plot, user can apply Fourier transform to the combined signal. The Fourier transform produces the frequency distribution of the individual signals from the combined signal. So the figure shows the separated spectrums corresponding to every column

Part C, D and E are mainly to simulate the process of reconstruct the two dimensional matrix.

www.manaraa.com

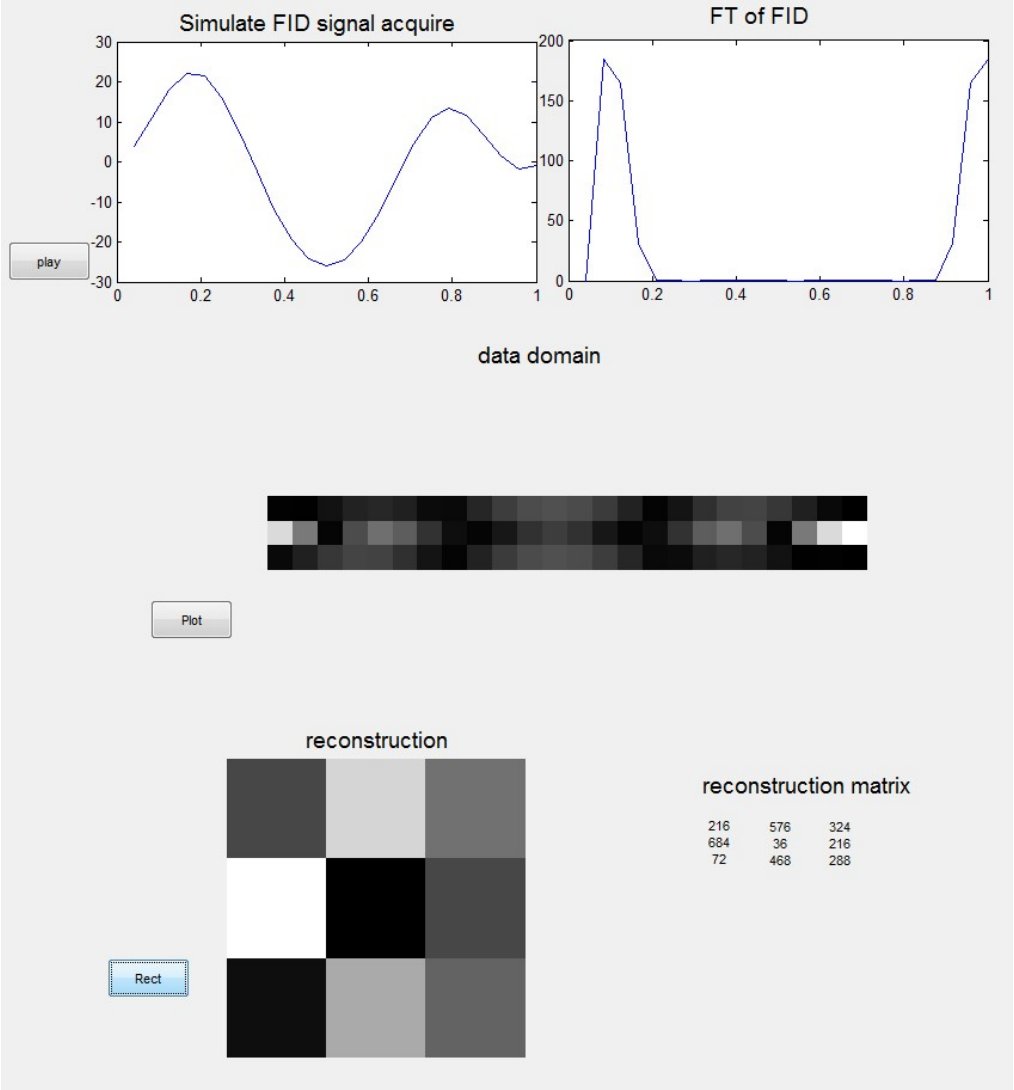

Figure 5. 4 These are Part C, Part D and Part E of the GUI tutorial. In Part C displays the simulated magnetic resonance signal in time domain and frequency domain. Part D is the result of data domain. Part E includes the reconstructed grayscale image and the matrix.

Part C simulates magnetic resonance signal received from the whole matrix (Eq.12) after spatial encoding and its Fourier transform result. This process will repeat for three times with a variable gradient G.

www.manaraa.com

$$combined\ signal = \iint signal(x,y)\, d_x d_y \qquad \text{Eq. 12}$$

$$= \iint \rho(x,y) * \mathrm{e}^{-i\gamma(B_0+G)t}\ d_x d_y$$

These three signals constitute the data space, as shown in part D. In part E, data space is used to reconstruct the original grayscale image and matrix by the application of Fourier transform.

Reconstruction Simulation

This GUI allows user to upload any image.

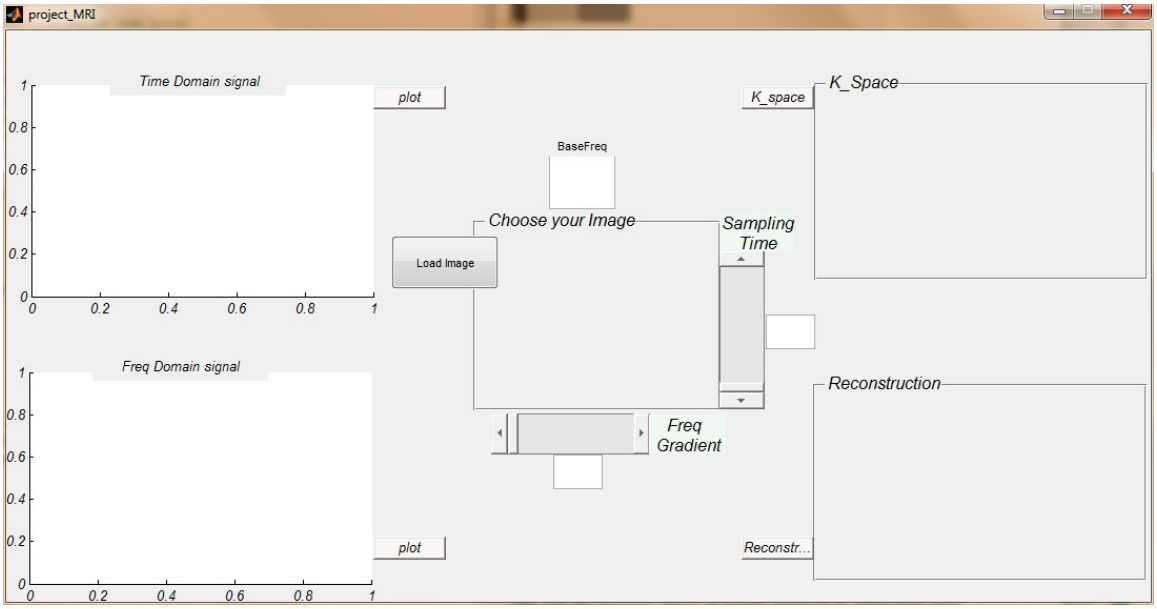

Figure 5. 5 This is reconstruction simulation GUI. User can choose the image and play the whole simulation process with the chosen image. User can see the simulated signal in time domain and frequency domain in the left side. K-space of the image and the reconstruction result are displayed in the right side.

On the left side, the first plot displays the simulated MR signal of the image in the time domain. The second plot is the corresponding result in frequency domain after Fourier

www.manaraa.com

transform. On the right side, the two plots shows simulated k-space and the reconstructed image.

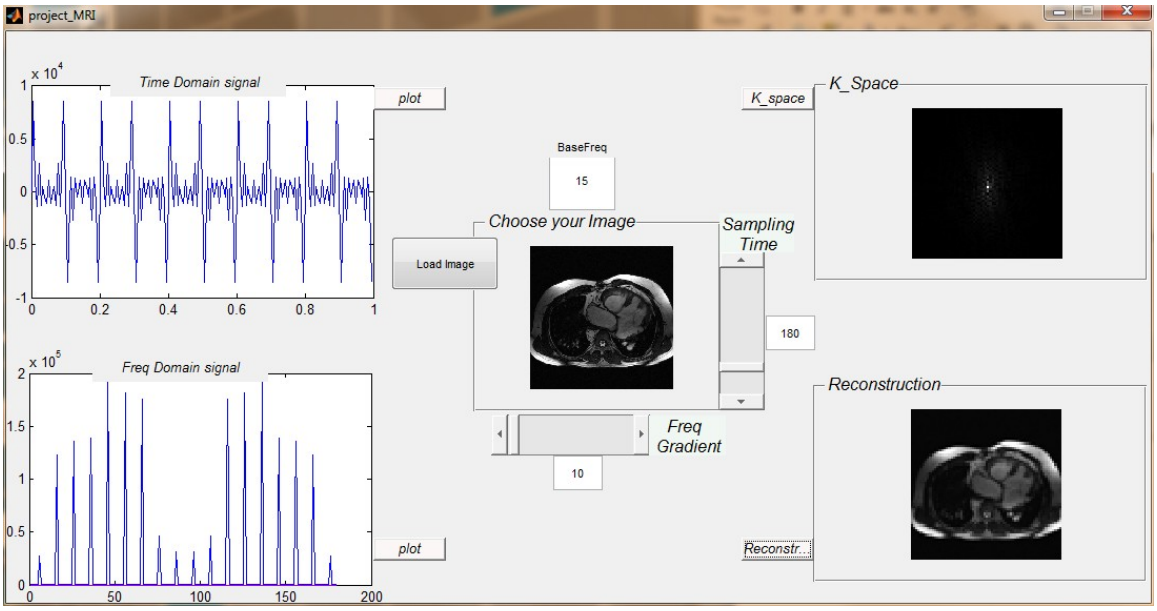

Figure 5. 6 This is an example with a stomach image. User can see the simulated signal in time domain and frequency domain in the left side. K-space of the image and the reconstruction result are displayed in the right side.

www.manaraa.com

Chapter 6 Conclusion

Since the principles of magnetic resonance imaging (MRI) are multi-disciplinary, it is difficult to learn the MRI system. In this research project, a MRI simulation system was cast in the laboratory environment to help the engineering students learn the basic principles of MRI. This MRI simulation system includes hardware system and software system. For the hardware system, an Earth's magnetic field nuclear magnetic resonance (EFNMR) system was set up. Base on this EFNMR system, MR signal acquisition and relaxation time weighted image can be simulated. For the software system, two graphical user interface based platforms were developed. The first one simulates the magnetic resonance signal, Fourier transform and magnetic gradient concepts. The second one lets users upload any image and simulates the two dimensional MRI image reconstruction.

The EFNMR system is a low cost substitute of real MRI, which is easily accessible to students in the laboratory. Through these experiments on the EFNMR, students can not only directly visualize the concepts but also practice the MRI knowledge. In the graphical user interface (GUI), user can adjust the relative input parameters of the MR signals and see the data space results. Through this interactive way, the tutorial GUI can effectively help students understand related magnetic resonance imaging principles and concepts.

As the EFNMR system is worked on the Earth's magnetic field, the pulse frequency is low and the nuclear magnetization is weak. The electric noises from the surround environment are high enough to disturb the magnetic resonance signal of this system. The further work is to design a shielding coil for the coil probe. This shielding coil could

www.manaraa.com

reduce the influence from the surround electric noises. Besides, other MRI experiments can be designed and realized in the system, such as proton density weighted image. In this research experiment, we only used the basic sample (water and copper sulfate solution). More complicated samples can be designed and tested.

The software simulation is based on the ideal noiseless condition in this research project, no relaxation process is considered. The further work is to simulate the situation with relaxation process. Besides more materials could be include, such as the simulation of Bloch equation which is very helpful to understand the evolution of the nuclear magnetization. Other imaging technique such as half Fourier imaging can be simulated.

All in all, with the further improvement, this MRI simulation system can cover more knowledge of MRI. This system can be a good tool to learn MRI.

www.manaraa.com

Reference

1. Geva, T., *Magnetic resonance imaging: Historical perspective.* Journal of Cardiovascular Magnetic Resonance, 2006. **8**(4): p. 573-580.

2. Roguin, A., *Nikola Tesla: The man behind the magnetic field unit.* Journal of Magnetic Resonance Imaging, 2004. **19**(3): p. 369-374.

3. Tubridy, N. and C.S. McKinstry, *Neuroradiological history: Sir Joseph Larmor and the basis of MRI physics.* Neuroradiology, 2000. **42**(11): p. 852-855.

4. Pound, R.V. and E.M. Purcell, *Measurement of magnetic resonance absorption by nuclear moments in a solid.* Physical Review, 1946. **69**(11-1): p. 681-681.

5. Purcell, E.M., H.C. Torrey, and R.V. Pound, *Resonance absorption by nuclear magnetic moments in a solid.* Physical Review, 1946. **69**(1-2): p. 37-38.

6. Bloch, F., *Nuclear induction.* Physical Review, 1946. **70**(7-8): p. 460-474.

7. Lauterbur, P.C., *Image formation by induced local interactions - Examples Employing Nuclear Magnetic-Resonance.* Nature, 1973. **242**(5394): p. 190-191.

8. Mansfield, P. and P.K. Grannell, *NMR diffraction in solids.* Journal of Physics C-Solid State Physics, 1973. **6**(22): p. L422-L426.

9. Kumar, A., D. Welti, and R.R. Ernst, *NMR Fourier zeugmatography.* Journal of Magnetic Resonance, 1975. **18**(1): p. 69-83.

10. Kumar, A., D. Welti, and R.R. Ernst, *Imaging of macroscopic objects by NMR Fourier zeugmatography.* Naturwissenschaften, 1975. **62**(1): p. 34-34.

11. Beyersdorff, D., et al., *MRI of prostate cancer at 1.5 and 3.0 T: Comparison of image quality in tumor detection and staging.* American Journal of Roentgenology, 2005. **185**(5): p. 1214-1220.

12. Greil, G.F., et al., *Gadolinium-enhanced three-dimensional magnetic resonance angiography of pulmonary and systemic venous anomalies.* Journal of the American College of Cardiology, 2002. **39**(2): p. 335-341.

13. Ogawa, S., et al., *Brain magnetic-resonance-imaging with contrast dependent on blood oxygenation.* Proceedings of the National Academy of Sciences of the United States of America, 1990. **87**(24): p. 9868-9872.

www.manaraa.com

14. Ogawa, S., et al., *Functional brain mapping by blood oxygenation level-dependent contrast magnetic-resonance-imaging - a comparison of signal characteristics with a biophysical model.* Biophysical Journal, 1993. **64**(3): p. 803-812.

15. Prince, M.R., et al., *Three-dimensional gadolinium-enhanced MR angiography of the thoracic aorta.* American Journal of Roentgenology, 1996. **166**(6): p. 1387-1397.

16. Prince, M.R., et al., *Breath-hold gadolinium-enhanced MR-angiography of the abdominal-aorta and its major branches.* Radiology, 1995. **197**(3): p. 785-792.

17. Lederman, R.J., et al., *Catheter-based endomyocardial injection with real-time magnetic resonance imaging.* Circulation, 2002. **105**(11): p. 1282-1284.

18. Liang, Z.-P., P.C. Lauterbur, and IEEE Engineering in Medicine and Biology Society., *Principles of magnetic resonance imaging : a signal processing perspective*. IEEE Press series in biomedical engineering2000, Bellingham, Wash.

19. Mezrich, R., *A perspective on K-space.* Radiology, 1995. **195**(2): p. 297-315.

20. Gossuin, Y., et al., *Physics of magnetic resonance imaging: from spin to pixel.* Journal of Physics D-Applied Physics, 2010. **43**(21).

21. Schenck, J.F., *Health and physiological effects of human exposure to whole-body four-tesla magnetic fields during MRI.* Ann N Y Acad Sci, 1992. **649**: p. 285-301.

22. Glover, P.M., *Interaction of MRI field gradients with the human body.* Physics in Medicine and Biology, 2009. **54**(21): p. R99-R115.

23. Kok, R.D., et al., *Absence of harmful effects of magnetic resonance exposure at 1.5 T in utero during the third trimester of pregnancy: a follow-up study.* Magnetic Resonance Imaging, 2004. **22**(6): p. 851-854.

24. Hinshaw, W.S. and A.H. Lent, *An introduction to NMR imaging: From the Bloch equation to the imaging equation.* Proceedings of the IEEE, 1983. **71**(3): p. 338-350.

25. Williams, J.E.C., *Superconducting Magnets for MRI.* IEEE Transactions on Nuclear Science, 1984. **31**(4): p. 994-1005.

26. Horowitz, A.L., *MRI physics for radiologists : a visual approach*. 3rd ed1995, New York: Springer-Verlag. xii, 180 p.

www.manaraa.com

27. Cosmus, T.C. and M. Parizh, *Advances in whole-body MRI magnets.* IEEE Transactions on Applied Superconductivity, 2011. **21**(3): p. 2104-2109.

28. Ray H.Hashemi, W.G.B., Christopher J.Lisanti, *MRI: The basics*. 2nd ed September 1, 2004: Lippincott Williams & Wilkins; 2nd edition (September 1, 2004). 353 pages.

29. Fox, S.I., *Human physiology*. 11th ed2009, Boston: McGraw-Hill Higher Education. xxiii, 808 p.

30. Prince, J.L. and J.M. Links, *Medical imaging signals and systems* 2006, Upper Saddle River, NJ: Pearson Prentice Hall.

31. Bernstein, M.A., K.F. King, and Z.J. Zhou, *Handbook of MRI pulse sequences* 2004, Amsterdam ; Boston: Academic Press. xxii,1017 p.

32. Robinson, J.N., et al., *Two-dimensional NMR spectroscopy in Earth's magnetic field.* Journal of Magnetic Resonance, 2006. **182**(2): p. 343-347.

33. Hamans, B.C., et al., *NMR at Earth's magnetic field using para-hydrogen induced polarization.* Journal of Magnetic Resonance, 2011. **212**(1): p. 224-228.

34. Callaghan, P.T. and M. Le Gros, *Nuclear spins in the Earth's magnetic field.* American Journal of Physics, 1982. **50**(8): p. 709-713 (1982).

35. Mohoric, A., et al., *Magnetic resonance imaging system based on Earth's magnetic field.* Instrumentation Science & Technology, 2004. **32**(6): p. 655-667.

36. Stepisnik, J., V. Erzen, and M. Kos, *NMR imaging in the earth's magnetic field.* Magn Reson Med, 1990. **15**(3): p. 386-91.

37. Halse, M.E. and P.T. Callaghan, *A dynamic nuclear polarization strategy for multi-dimensional Earth's field NMR spectroscopy.* Journal of Magnetic Resonance, 2008. **195**(2): p. 162-168.

38. Landis, C.S., et al., *Determination of the MRI contrast agent concentration time course in vivo following bolus injection: effect of equilibrium transcytolemmal water exchange.* Magn Reson Med, 2000. **44**(4): p. 563-74.

39. Naruse, S., et al., *Significance of proton relaxation time measurement in brain edema, cerebral infarction and brain tumors.* Magnetic Resonance Imaging, 1986. **4**(4): p. 293-304.

www.manaraa.com

40. Woessner, D.E., et al., *Numerical solution of the Bloch equations provides insights into the optimum design of PARACEST agents for MRI.* Magnetic Resonance in Medicine, 2005. **53**(4): p. 790-799.

41. Wehrli, F.W., et al., *Mechanisms of Contrast in NMR Imaging.* Journal of Computer Assisted Tomography, 1984. **8**(3): p. 369-380.

42. Spees, W.M., et al., *Water proton MR properties of human blood at 1.5 Tesla: Magnetic susceptibility, T-1, T-2, T-2* and non-Lorentzian signal behavior.* Magnetic Resonance in Medicine, 2001. **45**(4): p. 533-542.

43. David-Vaudey, E., et al., *T2 relaxation time measurements in osteoarthritis.* magnetic resonance imaging, 2004. **22**(5): p. 673-82.

44. Duncan, J.S., P. Bartlett, and G.J. Barker, *Technique for measuring hippocampal T2 relaxation time.* American Journal of Neuroradiology, 1996. **17**(10): p. 1805-1810.

45. D.I, H., *The solution of the bloch equations in the presence of a varying B1 field—An approach to selective pulse analysis.* Journal of Magnetic Resonance (1969), 1979. **35**(1): p. 69-86.

46. Nitz, W.R. and P. Reimer, *Contrast mechanisms in MR imaging.* Eur Radiol, 1999. **9**(6): p. 1032-46.

47. Lauterbur, P.C., *Image formation by induced local interactions: examples employing nuclear magnetic resonance.* Nature, 1973. **242**(5394): p. 190-191.

48. Cho, Z.H., et al., *Fourier transform nuclear magnetic resonance tomographic imaging.* Proceedings of the IEEE, 1982. **70**(10): p. 1152-1173.

49. Fessler, J.A., *Model-based image reconstruction for MRI.* IEEE Signal Processing Magazine, 2010. **27**(4): p. 81-89.

www.manaraa.com

APPENDIX

Magnetic Resonance Imaging Experiment Manuel

Purpose: To demonstrate the nuclear magnetic resonance phenomenon and relaxation time weighted contrast mechanism of Magnetic Resonance Imaging.

Equipment: a computer, a spectrometer and a three coil probe.

Samples: tap water and copper sulfate solution (Concentration is 660 uM).

Tasks: 1. To find the Larmor frequency of the water sample. 2. To acquire the nuclear magnetic resonance (NMR) signal from hydrogen, include free induction decay (FID) and echo. 3. Try to optimize the quality of the signal. 4. To measure the relaxation parameters T_1 and T_2. 5. To get relaxation time weighted imaging.

Experiment 1

Analyses B1 coil

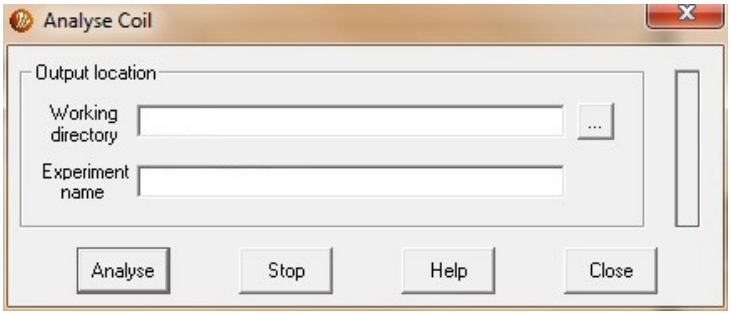

Figure 1 Analyses B1 coil

www.manaraa.com

1. Choose the "AnalyseCoil" macro. In working directory define the folder you want to save the experiment results. The format of experiment name is "experiment and date". For example, if this experiment is performed on April6th, 2012, its experiment name should be: AnalyCoil04062012.
2. Press the "Analyse" button to begin the experiment. In the result window, record the values of B1 coil capacitance and B1 coil induction.

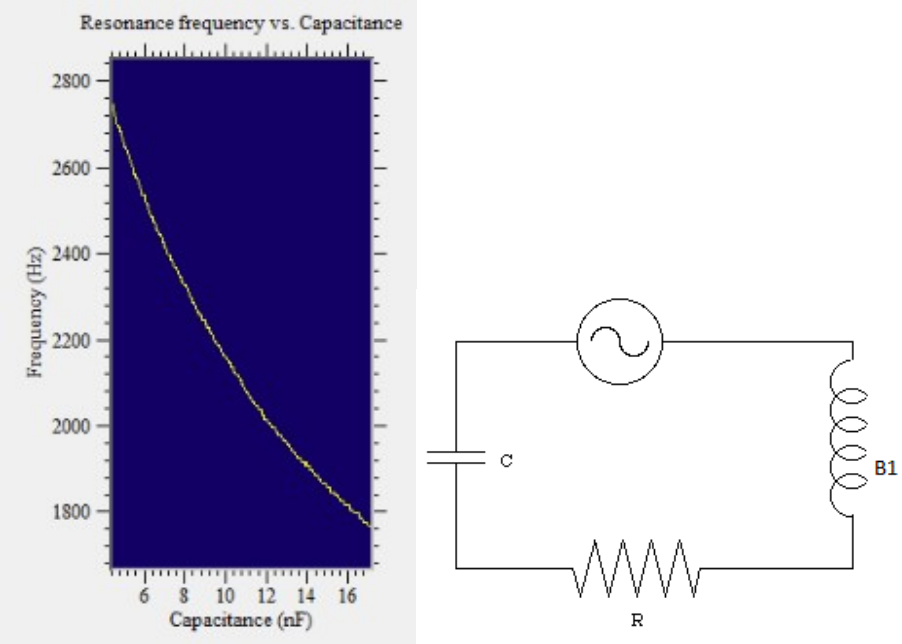

Figure 2 Experiment1 result and LCR circuit

3. Briefly describe how the LCR circuit on the right works. The left plot is one of the results of this experiment, based on it describe the relationship between the capacitance and resonance frequency of the B1 coil.

Note: in this coil probe, the B1 coil is tuned by this LCR circuit.

www.manaraa.com

Experiment 2

Find the Larmor frequency

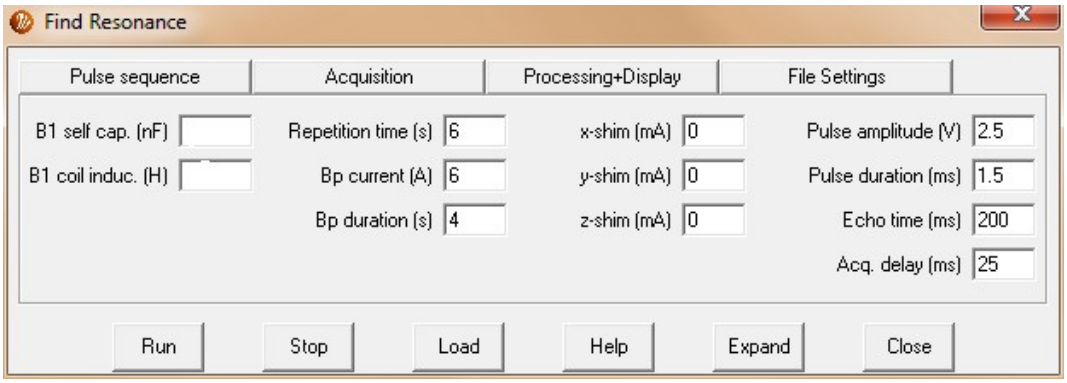

Figure 3 Find Resonance frequency

1. Put the water sample in the coil probe. Choose the "Auto Tune" macro. Fill in the B1 capacitance and B1 induction values in the window above.
2. You will get the below image. Read out the capacitance value that corresponding to the most colorful region.

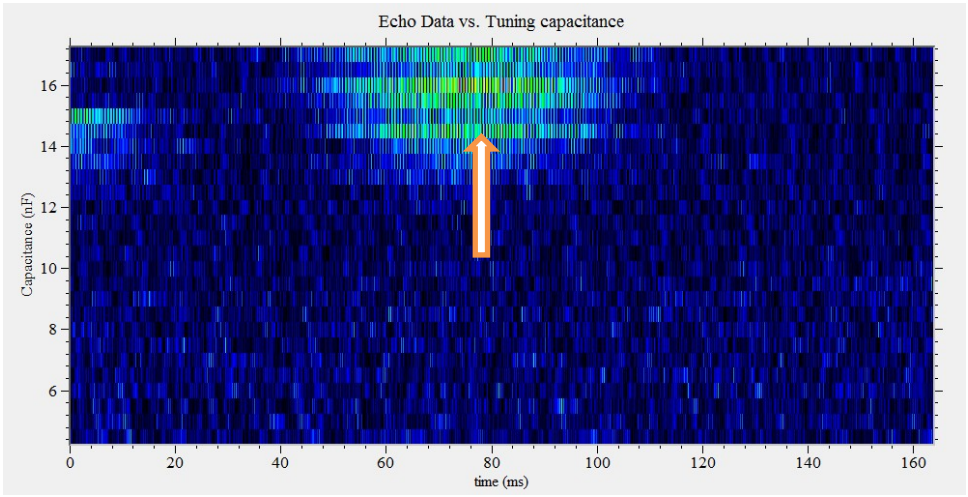

Figure 4 Experiment 2 result

www.manaraa.com

3. In the result window find the "b1 frequency" value that corresponding to the capacitance value get above. Record these two values.
4. Briefly describe what are the b1 frequency value and its relationship with capacitance value.

Experiment 3

Get the free induction decay (FID) signal

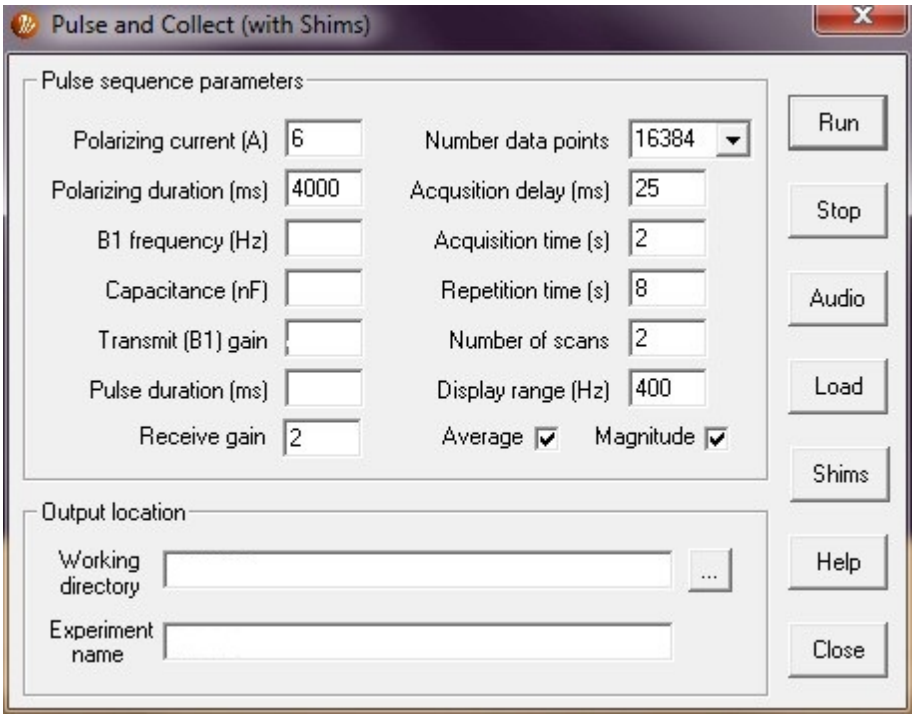

Figure 5 Acquire free induction decay

1. Put the water sample in the coil probe. Choose the "pulse and collect" macro. Fill in your B1 frequency and capacitance value. The transmit gain is recommended as 2 and pulse duration can be around 1. The other parameters can be the same.

www.manaraa.com

2. Click run to perform this experiment, the result is as below.

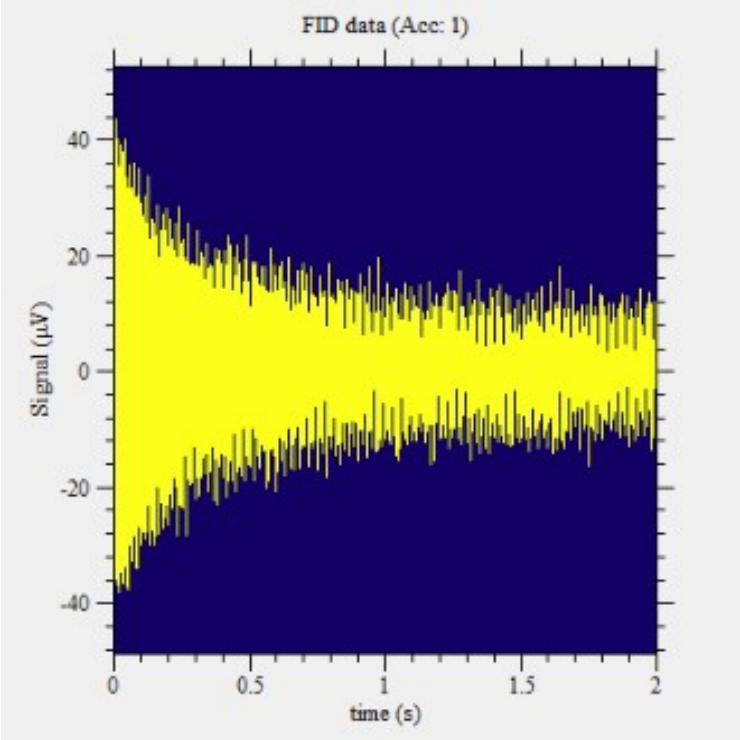

Figure 6 Experiment 3 result

3. Try to change the frequency value and capacitance value and analysis the result.
4. Try to change the value of pulse duration and analysis the results. Tip: the pulse duration parameter determines the time to apply the excitation pulse.

www.manaraa.com

Experiment 4

Improve the homogeneity of the magnetic field

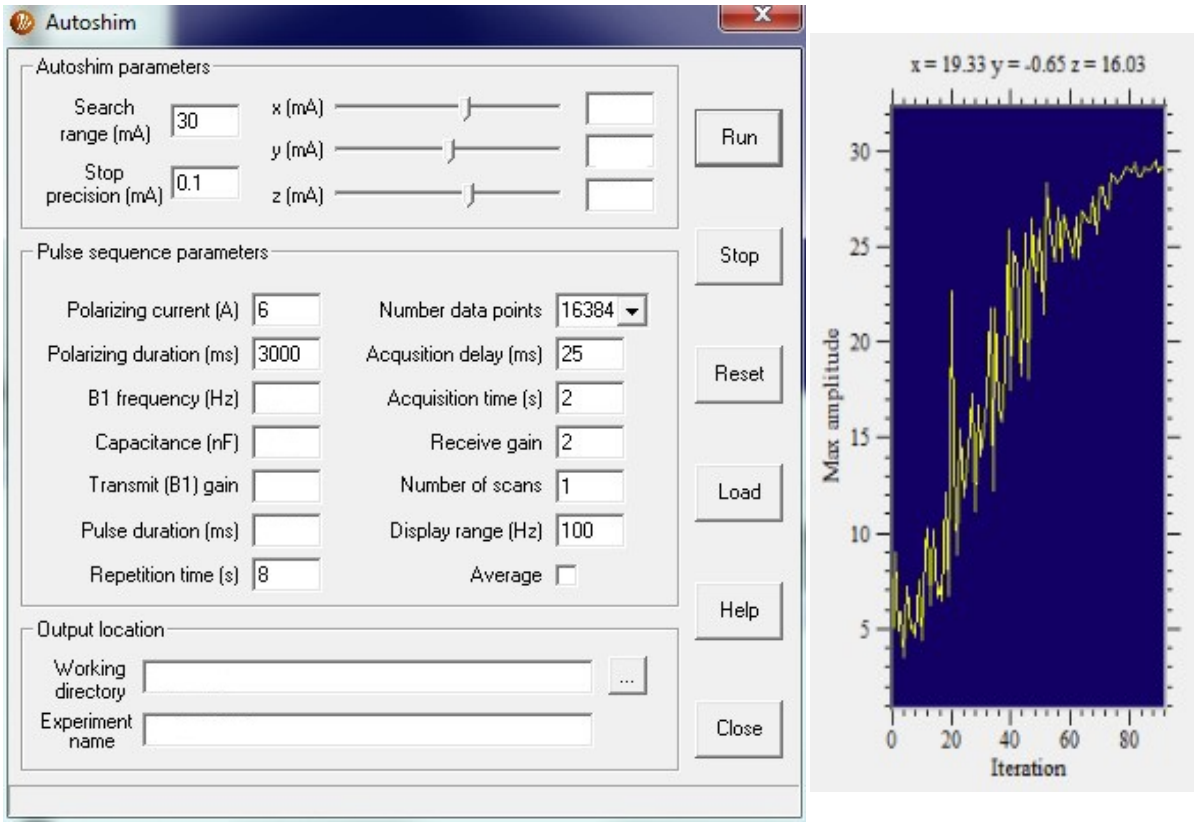

Figure 7 Experiment 4 and result

1. Put the water sample in the coil probe. Choose the "Auto shim" macro. Fill in your B1 frequency and capacitance value.
2. Fill in the transmit gain parameter as 2 and choose the pulse duration value that you think can get the best FID signal.
3. Click run to perform this experiment. This experiment will take about 10 minutes. You will get a result figure as right figure.

www.manaraa.com

4. As the experiment finish, repeat the "pulse and collect" experiment to see if the FID signal is better.
5. Consider how this experiment help improve the FID signal. Briefly describe the reason.

Experiment 5

Get the B1 duration parameters

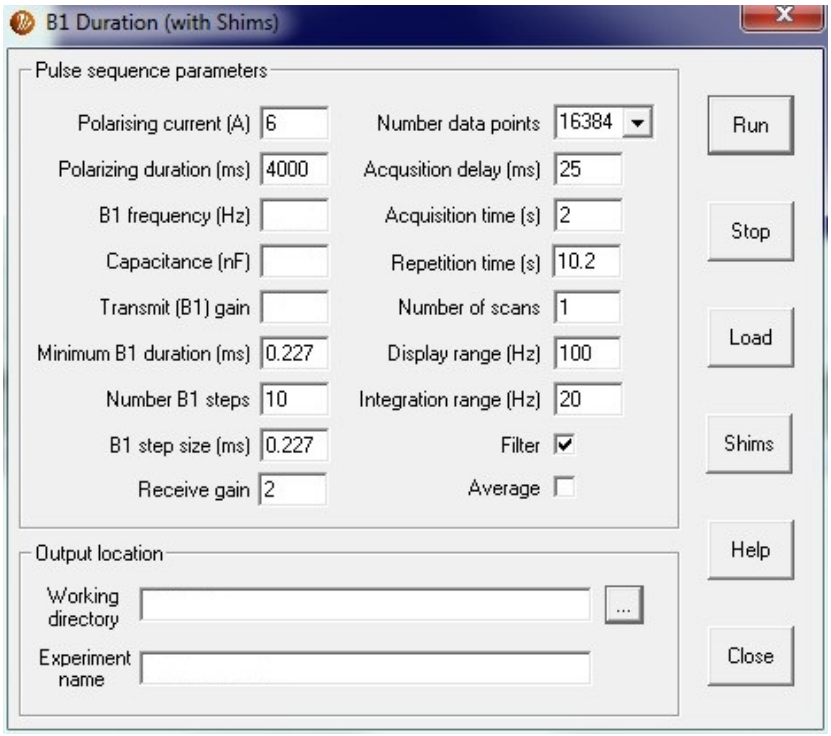

Figure 8 Get the B1 duration parameters

1. Put the water sample in the coil probe. Choose the "B1 Duration" macro. Fill in your B1 frequency and capacitance parameters and run the experiment.

www.manaraa.com

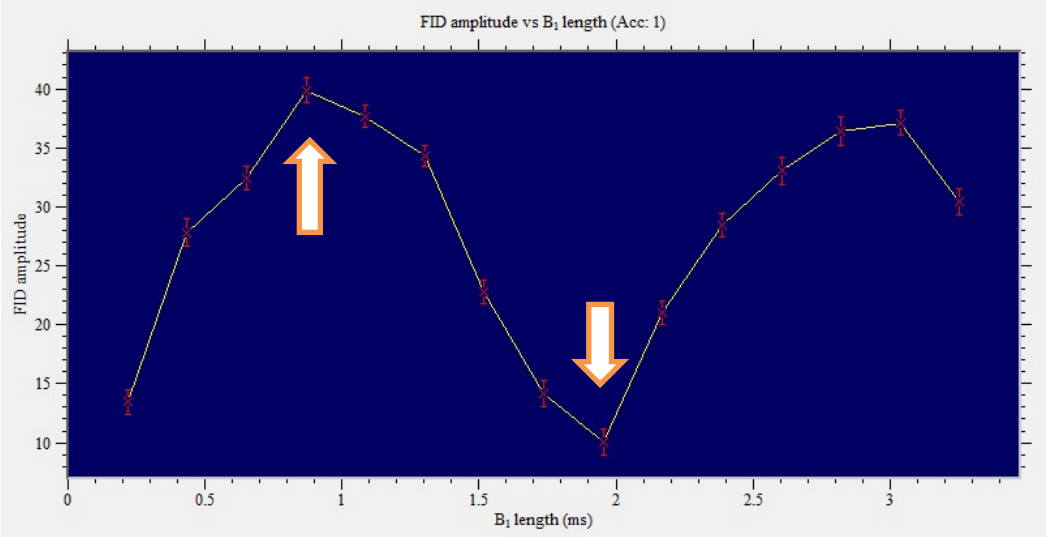

Figure 9 Experiment 5 result

2. Run the experiment and you will get the result figure as above. Readout the b1 length that corresponding to the first maximum FID amplitude as 90 pulse duration and the B1 length corresponding to the following minimum FID amplitude as the 180 pulse duration.
3. With your 90 pulse duration and 180 pulse duration repeat the "pulse and collect" experiment. Get the results with pulse duration parameter equals to 90 pulse duration and 180 pulse duration separately. Compare the results and analysis it.

www.manaraa.com

Experiment 6

Get the spin echo signal

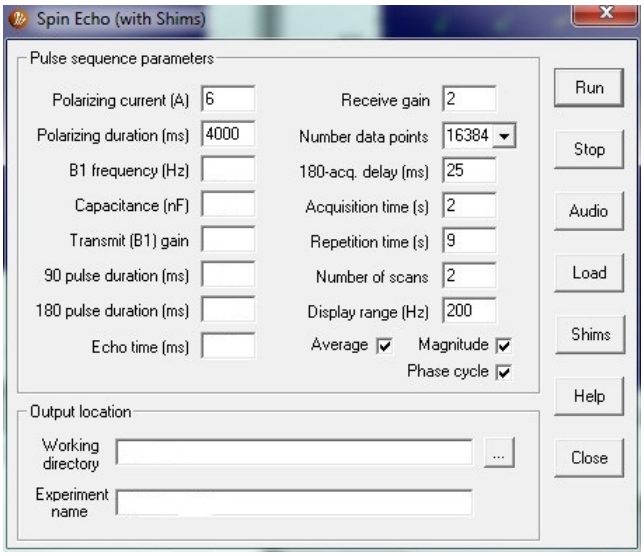

Figure 10 Acquire the spin echo signal

1. Put the water sample in the coil probe. Choose “spin echo” macro. Fill in your B1 frequency, capacitance, 90 pulse duration and 180 pulse duration parameters.
2. The echo time value should be bigger than the decay time of FID signal. You can obtain the decay time of the FID signal from the “pulse and collect” experiment.

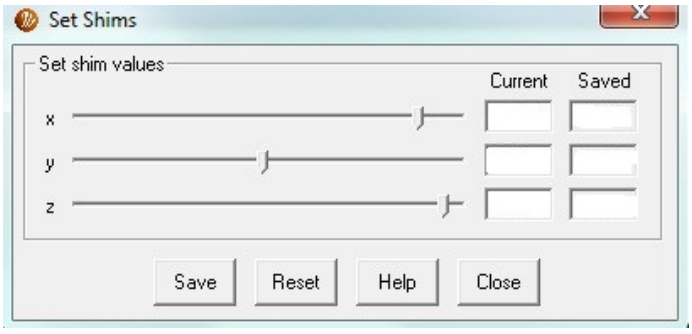

Figure 11 Deshim process

www.manaraa.com

3. Click the “Shims” bottom you can get the above figure. Try to change the value of X or Y or Z by adjusts the slider. This process is called “deshim”.You only need to change one from X, Y and Z. Then repeat this experiment, compare the results and analysis it.
4. Click run to perform this experiment and see the result. Figure below is an example result.

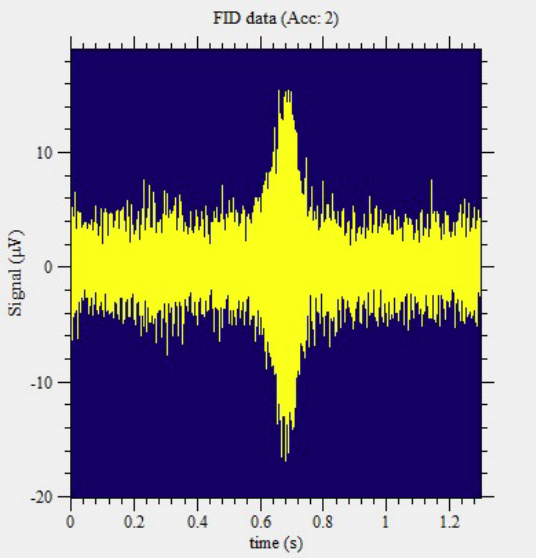

Figure 12 Experiment 6 result

www.manaraa.com

Experiment 7

To measure the spin-lattice relaxation time T_1

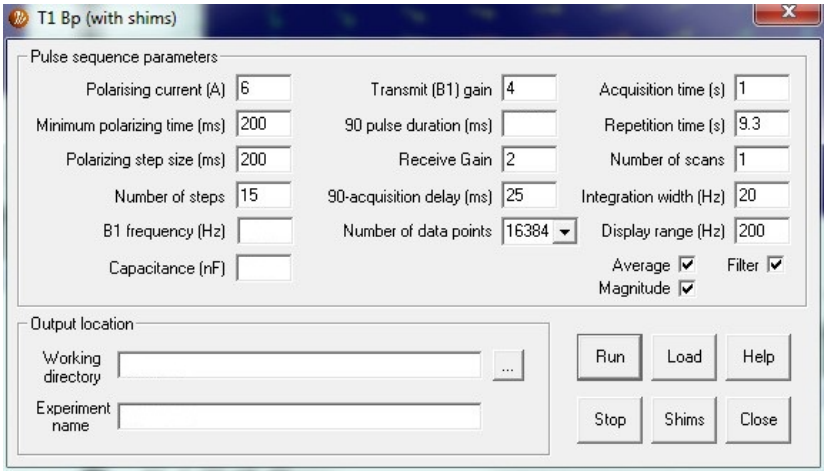

Figure 13 Relaxation time measurement experiment

1. Put the water sample in the coil probe. Choose the "$T_1 B_p$" macro. Fill in your B1 frequency, Capacitance and 90 pulse duration parameters.
2. Click run to perform the experiment and record the data results. After the experiment you will get the result figure as below. The below figure provides the T_1 value and T_1 curve of water sample.
3. Change the water sample to copper sulfate solution and repeat this experiment. Record the T_1 value for both water and copper sulfate solution.

www.manaraa.com

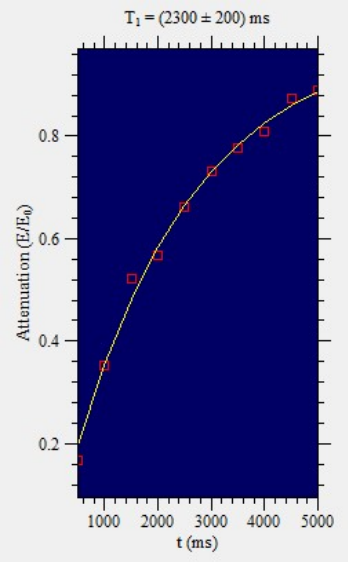

Figure 14 Experiment 7 result

Experiment 8

To measure the spin-lattice relaxation time T_2

1. Put the water sample in the coil probe. Choose the "T_2" macro. Fill in your B1 frequency, Capacitance and 90 pulse duration parameters.

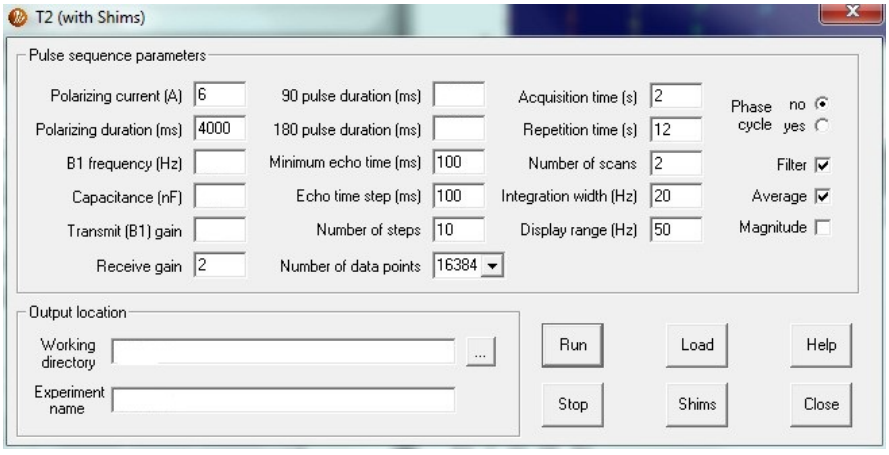

Figure 15 Relaxation time measurement experiment

www.manaraa.com

2. Before run this experiment perform the deshim process. Click run to perform the experiment and record the data results. After the experiment you will get the result figure as below. The below figure provides the T_2 value and T_2 curve of water sample.
3. Change the water sample to copper sulfate solution and repeat this experiment. Record the T_2 value for both water and copper sulfate solution.

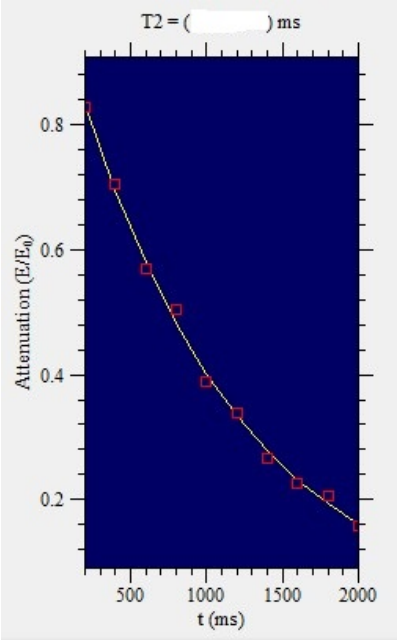

Figure 16 Experiment 8 result

Experiment 9

To obtain relaxation time weighted imaging

www.manaraa.com

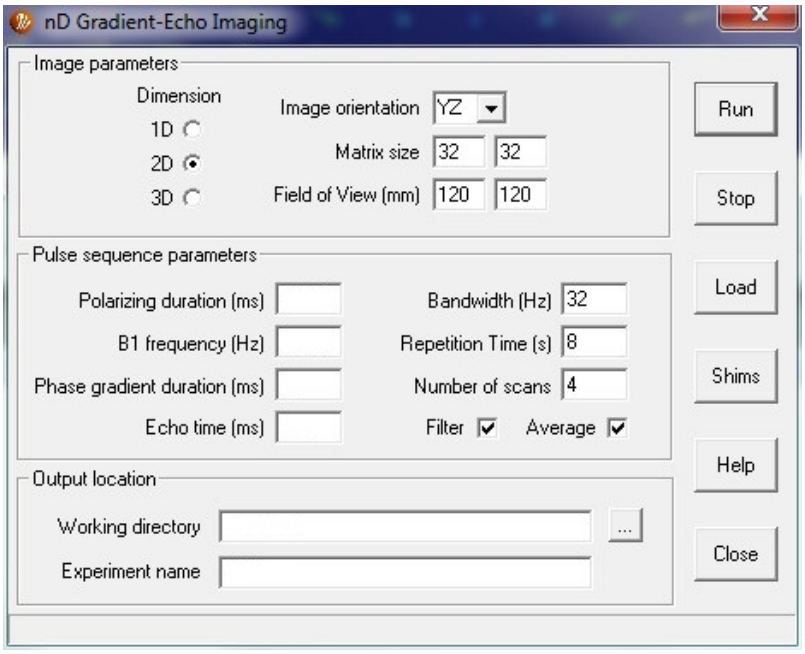

Figure 17 Gradient echo imaging

1. Prepare a sample compose by two small bottle, one is water and the other is copper sulfate solution. You have already obtained the relaxation time values of these two samples.
2. Choose the "Gradient Echo Imaging". Review the principles of relaxation time weighted imaging.
3. T_1 Weighted imaging: base on the T_2 curve of the two samples choose the echo time as small as possible to eliminate the T_2 effect. Base on the T_1 curve, choose the polarizing duration value that produce the most significant different between the two samples. You can also repeat the experiment with different polarization duration value. The below figure is one example.

www.manaraa.com

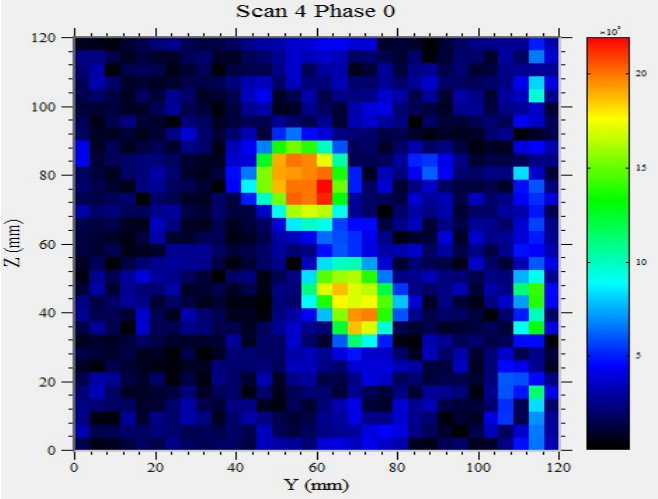

Figure 18 Experiment 9 result-1

4. T_2 Weighted imaging: base on the T_1 curve choose the polarization value that have the least different between the two samples. Base on the T_2 curve choose the echo time that generate the most significant different between the two samples. You can repeat this experiment with different timing parameters. The below figure is one example.

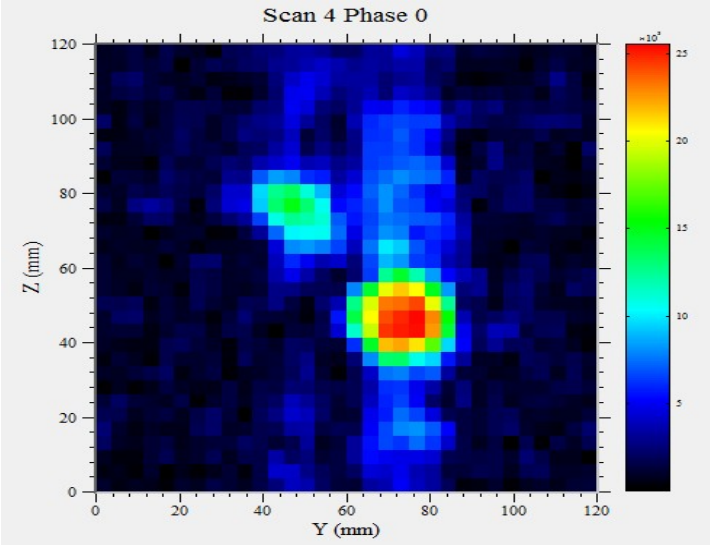

Figure 19 Experiment 9 result-2

www.manaraa.com